A Large-Scale Genetic Screen in Arabidopsis to Identify Genes Involved in Pollen Exine Production[1][C][W][OA]

Anna A. Dobritsa*, Aliza Geanconteri, Jay Shrestha, Ann Carlson, Nicholas Kooyers[2], Daniel Coerper[3], Ewa Urbanczyk-Wochniak[4], Bennie J. Bench[5], Lloyd W. Sumner, Robert Swanson, and Daphne Preuss[6]

Department of Molecular Genetics and Cell Biology, University of Chicago, Chicago, Illinois 60637 (A.A.D., A.G., J.S., D.C., D.P.); Biology Department, Valparaiso University, Valparaiso, Indiana 46383 (A.C., N.K., R.S.); and Plant Biology Division, Samuel Roberts Noble Foundation, Ardmore, Oklahoma 73401 (E.U.-W., B.J.B., L.W.S.)

Exine, the outer plant pollen wall, has elaborate species-specific patterns, provides a protective barrier for male gametophytes, and serves as a mediator of strong and species-specific pollen-stigma adhesion. Exine is made of sporopollenin, a material remarkable for its strength, elasticity, and chemical durability. The chemical nature of sporopollenin, as well as the developmental mechanisms that govern its assembly into diverse patterns in different species, are poorly understood. Here, we describe a simple yet effective genetic screen in Arabidopsis (*Arabidopsis thaliana*) that was undertaken to advance our understanding of sporopollenin synthesis and exine assembly. This screen led to the recovery of mutants with a variety of defects in exine structure, including multiple mutants with novel phenotypes. Fifty-six mutants were selected for further characterization and are reported here. In 14 cases, we have mapped defects to specific genes, including four with previously demonstrated or suggested roles in exine development (*MALE STERILITY2*, *CYP703A2*, *ANTHER-SPECIFIC PROTEIN6*, *TETRAKETIDE α-PYRONE REDUCTASE/DIHYDROFLAVONOL-4-REDUCTASE-LIKE1*), and a number of genes that have not been implicated in exine production prior to this screen (among them, fatty acid ω-hydroxylase *CYP704B1*, putative glycosyl transferases At1g27600 and At1g33430, 4-coumarate-coenzyme A ligase *4CL3*, polygalacturonase *QUARTET3*, novel gene At5g58100, and nucleotide-sugar transporter At5g65000). Our study illustrates that morphological screens of pollen can be extremely fruitful in identifying previously unknown exine genes and lays the foundation for biochemical, developmental, and evolutionary studies of exine production.

Plants have evolved remarkable and unique pollen walls. The pollen surface consists of inner (intine) and outer (exine) walls, coated with a lipid- and protein-rich extracellular matrix (the pollen coat; Fig. 1A). Exine provides several important functions to pollen grains: (1) it protects gametophytes in harsh environments and serves as a barrier against various physical and chemical factors and biological pathogens (Scott, 1994); (2) it helps with pollen dispersal and cross-pollination in some species (Faegri and van der Pijl, 1979); and (3) it enables stigma cells to capture the most appropriate pollen grains by providing species-specific factors for pollen-stigma recognition and adhesion (Zinkl et al., 1999).

There is an astonishing variety of exine patterns across different plant species, yet the overall pollen wall architecture is conserved among angiosperms. Often, the outer part of exine is elaborate, with radially directed rods (baculae) with expanded ends that often fuse to form patterned walls (muri) and a roof (tectum; Fig. 1A). Most pollen walls contain characteristic apertures or pores, thought to allow pollen tube emergence and changes in grain volume (Wodehouse, 1935; Heslop-Harrison, 1979a; Muller, 1979; Blackmore and Barnes, 1986; Katifori et al., 2010); these regions are often covered only by intine. The uniform appearance of apertures within a species indicates the presence of mechanisms that specify sites where exine is not deposited or is reduced. In fact, in many species, the aperture number and positions are genetically determined and tightly controlled: for example, lily (*Lilium longiflorum*) pollen has a single aperture that always develops at the tetrad perimeter (Heslop-Harrison, 1968a), and Arabidopsis (*Arabidopsis thaliana*) grains, like those of

[1] This work was supported by the National Science Foundation (2010 Project grant no. MCB–0520283 to L.W.S., R.S., and D.P.).

[2] Present address: Department of Biology, Washington University, St. Louis, MO 63130.

[3] Present address: Department of Microbiology and Immunology, Loyola University Medical Center, Maywood, IL 60153.

[4] Present address: Monsanto Co., St. Louis, MO 63167.

[5] Present address: Food Safety and Research Laboratory, Tyson Foods, Inc., Springdale, AR 72762.

[6] Present address: Chromatin, Inc., Chicago, IL 60616.

* Corresponding author; e-mail dobritsa@uchicago.edu.

The author responsible for distribution of materials integral to the findings presented in this article in accordance with the policy described in the Instructions for Authors (www.plantphysiol.org) is: Anna A. Dobritsa (dobritsa@uchicago.edu).

[C] Some figures in this article are displayed in color online but in black and white in the print edition.

[W] The online version of this article contains Web-only data.

[OA] Open Access articles can be viewed online without a subscription.

www.plantphysiol.org/cgi/doi/10.1104/pp.111.179523

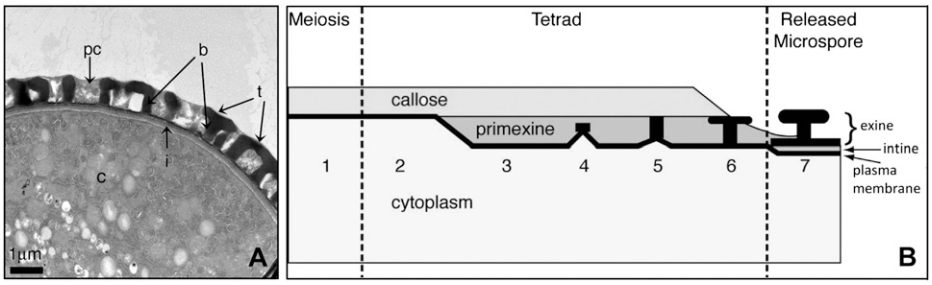

Figure 1. Plants have complex pollen walls. A, Transmission electron micrograph of a cross-section of Arabidopsis pollen. b, Baculae of exine; c, pollen grain cytoplasm; i, intine; pc, pollen coat; t, tectum of exine. B, Stages of exine assembly during microspore development (adapted from Scott [1994] and Paxson-Sowders et al. [1997]). Stage 1, pattern gene transcription and callose deposition; stage 2, patterning specifications; stage 3, primexine synthesis; stage 4, probaculae development; stage 5, protosporopollenin deposition; stage 6, callose removal; stage 7, sporopollenin strengthening and intine synthesis initiation.

many other eudicots, contain three apertures arranged in a radially symmetrical fashion.

Exine is made of sporopollenin, a tough and chemically inert biopolymer. The chemical resistance of sporopollenin makes it a formidable challenge to deduce its structure. While its precise chemical structure remains unclear, chemical analysis suggested that sporopollenin is made of phenolics, fatty acids, and alkanes (Guilford et al., 1988; Ahlers et al., 1999, 2000; Wiermann et al., 2001). The synthesis and patterning of exine are generated through the combined activities of factors in both developing microspores that will become pollen grains (or in microspore mother cells) and in tapetum, a diploid secretory tissue that lines the anthers and surrounds the microspores. Tapetum is responsible for the synthesis of most of the sporopollenin materials (Piffanelli et al., 1998; Scott et al., 2004).

The precursor of exine (primexine) is synthesized just after meiosis II and is deposited onto the microspore plasma membrane, under a layer of callose (β-1,3 glucan) that temporarily separates microspores (Owen and Makaroff, 1995; Paxson-Sowders et al., 1997; for stages of exine assembly, see Fig. 1B). When callose wall deposition around the microspore mother cell and developing microspores is prevented either by premature activation of a β-1,3 glucanase that degrades callose (Worrall et al., 1992) or by mutations in a callose synthase (Dong et al., 2005; Nishikawa et al., 2005), the resulting pollen grains have severe defects in exine sculpting.

Primexine is made primarily of polysaccharides and acts as a loose scaffold for the attachment of sporopollenin monomers, resulting in partially polymerized protosporopollenin (Heslop-Harrison, 1968b). The genes that determine species-specific primexine patterns are likely transcribed within the diploid nucleus of a premeiotic microspore mother cell, and the pattern information is then inherited by microspores. Exine patterns are specified early in pollen development, with the accumulation of sporopollenin monomers over sites where baculae will appear (Heslop-Harrison, 1971; Sheldon and Dickinson, 1983). Ultimately, the number of baculae and the extent of their fusion determine exine patterns; for example, if the connections are minimal, the pattern may be reticulate, whereas additional connections can result in a smooth surface. Centrifugation experiments have shown that exine patterning can be perturbed during the early meiotic prophase (Sheldon and Dickinson, 1983) and that the patterning also requires coordination between the pollen plasma membrane and its underlying cytoskeleton, vesicles, and endoplasmic reticulum (ER; Dickinson and Sheldon, 1986; Takahashi and Skvarla, 1991; Fitzgerald and Knox, 1995; Perez-Munoz et al., 1995; Paxson-Sowders et al., 2001).

The study of pollen wall development is currently gaining momentum with the identification of a growing number of genes important for exine production and sporopollenin synthesis (Aarts et al., 1997; Paxson-Sowders et al., 2001; Ariizumi et al., 2003, 2004; Dong et al., 2005; Nishikawa et al., 2005; Morant et al., 2007; Guan et al., 2008; Suzuki et al., 2008; de Azevedo Souza et al., 2009; Dobritsa et al., 2009a, 2009b, 2010; Tang et al., 2009; Grienenberger et al., 2010; Kim et al., 2010). Among the phenotypes of the corresponding Arabidopsis mutants are absence of exine, abnormally low sporopollenin level, not fully polymerized sporopollenin, and changes in exine patterns. Several of the genes (*MALE STERILITY2* [*MS2*], cytochromes P450 *CYP703A2* and *CYP704B1*, *ACYL-COENZYME A SYNTHETHASE5* [*ACOS5*], *FACELESS POLLEN1* [*FLP1*], *NO EXINE FORMATION1* [*NEF1*], *LESS ADHESIVE POLLEN/POLYKETIDE SYNTHASE* [*LAP5/PKSB* and *LAP6/PKSA*], and *TETRAKETIDE α-PYRONE REDUCTASE* [*TKPR1/DRL1* and *TKPR2/CCRL6*]) participate in fatty acid modification or accumulation (Aarts et al., 1997; Ariizumi et al., 2003, 2004; Morant et al., 2007; de Azevedo Souza et al., 2009; Doan et al., 2009; Dobritsa et al., 2009b; Grienenberger et al., 2010; Kim et al., 2010), highlighting the role of this pathway in exine synthesis. The *DEFECTIVE EXINE1* (*DEX1*) gene was suggested to contribute to exine assembly and encodes a predicted membrane-associated protein with similarity to animal integrins. DEX1 appears to interact with the plasma membrane to nucleate sporopollenin

deposition (Paxson-Sowders et al., 2001), and in *dex1* mutants, primexine deposition is significantly reduced, sporopollenin is randomly deposited on microspores, and the microspores are ultimately degraded. The *RUPTURED POLLEN GRAIN1* (*RPG1*) gene encodes a seven-transmembrane-domain protein that localizes to the plasma membrane of microsporocytes (Guan et al., 2008). Mutations in this gene affect plasma membrane structure and primexine deposition and lead to irregular exine structure and microspore collapse (Guan et al., 2008).

Recently, the in silico approach was found to be a productive way for identifying new genes involved in sporopollenin synthesis or transport (Grienenberger et al., 2010; Kim et al., 2010; Quilichini et al., 2010): several of the genes implicated in this process have a very high coexpression correlation and are expressed together only in anthers at a particular stage of microspore development (Morant et al., 2007; Dobritsa et al., 2009b, 2010; Grienenberger et al., 2010; Kim et al., 2010; Quilichini et al., 2010).

Yet, despite the progress in the identification of several exine genes, it is clear that many other yet unknown players are involved in the complex process of exine production and its assembly into elaborate patterns. Some of the known exine genes do not have the distinct expression pattern associated with sporopollenin synthesis genes. Therefore, the traditional genetic approaches remain invaluable for the identification of members of the genetic network required for the biosynthesis, transport, and assembly of exine components. However, because genetic screens required visualization of minute exine details on tiny pollen grains and were expected to be very labor intensive, such screens have not been widely used in the past. Previously, a genetic screen has been performed using scanning electron microscopy to search for mutants (*kaonashi* [*kns*] mutants) with defective exine patterning (Suzuki et al., 2008). Twelve mutants that form at least five complementation groups were identified in this screen. One of them (*kns2*) affects exine pattern by increasing baculae density and has defects in a gene encoding a Suc phosphate synthase, the enzyme that catalyzes the rate-limiting step in Suc biosynthesis (Suzuki et al., 2008). It remains to be determined which genes are affected in the other *kns* mutants.

Here, we describe a large-scale genetic screen in Arabidopsis that aimed to identify genes involved in exine development using a novel, and simpler, screening approach. We screened for anthers and pollen that at low magnification (dissection microscope level) showed visible defects. We screened approximately 16,000 lines with random T-DNA insertions and used reverse genetics on a collection of mutations in 49 exine candidate genes. A secondary screen at a higher resolution (confocal microscope level) was then applied to the promising mutants to identify the ones with true exine defects. We isolated multiple mutants with abnormal exines that exhibited a large variety of phenotypes. These ranged from a complete lack of exine to a loss of the net-like structure, changes in the thickness of exine wall, irregular exine patterning, abnormal number and position of apertures, changes in the sizes of lacunae on the exine surface to exine that appeared morphologically normal yet demonstrated an altered autofluorescence spectrum, suggesting a change in its composition. We describe 49 mutants (some of which were found to be allelic) isolated through the forward genetic screen and seven mutants isolated through the reverse genetic screen. Through both approaches, we identified 14 genes, 10 of which to our knowledge have not been previously implicated in exine production.

RESULTS

Forward Genetic Screen

While characterizing and mapping several mutations that cause defects in exine structure (Nishikawa et al., 2005; Dobritsa et al., 2009a, 2010), we noticed that exine abnormalities, which can only be visualized using high-resolution microscopy, often also showed defects in anther and pollen morphology that can be easily detected using low-magnification standard dissecting stereomicroscopes. Therefore, we used low-magnification microscopy to perform a genetic screen for mutants with various morphological abnormalities in pollen and anthers. We used 179 pools of 100 lines from the Arabidopsis SALK T-DNA collection (Alonso et al., 2003) and screened approximately 16,000 different lines. The phenotypes that were selected in the primary screen included (1) abnormal anthers (e.g. brown, shriveled, glossy, or with little visible pollen), (2) pollen that exhibited unusually strong adherence to anthers and was not as easily shed as pollen of wild-type plants, (3) pollen that was released as aggregates and clumps and not as individual pollen grains, (4) pollen that had unusual size and/or shape (e.g. bigger or smaller than the wild type, round versus normally oblong), color (e.g. white or brown versus wild-type yellow), or light reflection (glossy or translucent versus wild-type matte), and (5) fertility defects that were combined with visible pollen or anther defects. As a result of this broadly defined primary screen, we identified 495 mutant candidates. Often, however, we found multiple mutants with identical or very similar phenotypes within a group of plants derived from a single set of pooled SALK lines, indicating that many of the mutant candidates from the same pool were likely siblings. Usually, only one or two of the lines with identical phenotypes derived from the same pool were subjected to further analysis. Therefore, we estimated that we had identified approximately 213 different mutant lines.

Based on the most obvious morphological defects visible at low magnification, we placed mutants into five primary-screen classes: (1) glossy and/or sticky

pollen that is not easily released from the anthers (approximately 82 lines; Supplemental Fig. S1); (2) round pollen (approximately 17 lines); (3) little or no pollen produced (this phenotype was usually associated with sterility or reduction in fertility; approximately 48 lines); (4) large and square pollen (approximately 30 lines); and (5) irregular-size pollen produced by the same anther (approximately 36 lines; Fig. 2).

Initially, the screen also included assessment of the morphology of unhydrated pollen at higher magnification. This revealed that shapes of the mutant pollen grains were often significantly distorted (Fig. 3). It also indicated that mutants grouped together in the same primary-screen class (e.g. glossy and/or sticky pollen) sometimes had noticeably different pollen phenotypes when observed with a higher magnification (Fig. 3).

Reverse Genetic Screen

Prior to the start of our screen, the chemical analysis of sporopollenin (Guilford et al., 1988; Ahlers et al., 1999, 2000; Wiermann et al., 2001) and a small set of available exine mutants (Aarts et al., 1997; Ariizumi et al., 2003; Dong et al., 2005; Nishikawa et al., 2005; Morant et al., 2007) provided evidence that biosynthetic pathways that produce fatty acids, phenylpropanoids, and some other small molecules are important for exine synthesis. Therefore, we also screened mutants disrupted in 49 candidate genes using the same visual approach as described above (Fig. 2). We targeted genes encoding enzymes in the two pathways with the strong chemical and/or genetic evidence for a role in exine formation (fatty acid and phenylpropanoid), genes encoding enzymes from the pathways with controversial roles in exine synthesis (flavonoid and carotenoid), as well as a number of genes that are predominantly expressed in developing Arabidopsis anthers or are homologs of anther-specific genes from other plants. The mutants came primarily from the SALK and SAIL (Sessions et al., 2002) T-DNA collections (Table I; Supplemental Tables S1 and S2). Our analysis was limited by the availability of mutations in regions where they were likely to affect gene functions.

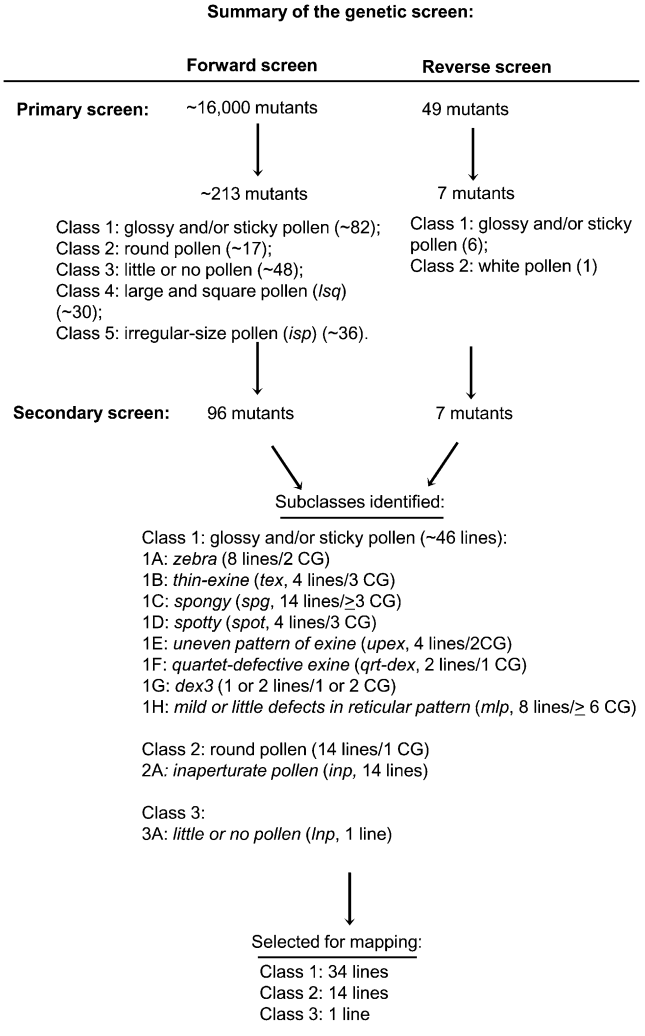

Figure 2. Summary of the genetic screen. CG, Number of genetic complementation groups formed by mutants in a phenotypic subclass.

We found seven genes in which mutations affected pollen or anther morphology (At1g33430, At1g65060, A1g69500, At2g19070, At3g28780, At4g14080, and At5g13930; Table I). For 19 genes, no morphological changes in the anthers or pollen were observed, despite the presence of homozygous insertions in their open reading frames or 5′ untranslated regions (Supplemental Table S1). For the rest of the genes (Supplemental Table S2), no obvious morphological changes were found. However, the results were inconclusive, usually because the insertion locations were in noncoding regions.

Of the genes that affected pollen or anther morphology, six of the seven mutants produced pollen that looked glossy and/or adhered more tightly to anthers (glossy and/or sticky pollen). These six genes have predicted anther-specific expression or are expressed in the buds at the stages of exine development (Table I). The seventh, an insertion in At5g13930/*TT4*, a gene for chalcone synthase (CHS) that plays a key role in the flavonoid biosynthesis and is not anther specific, did not have the glossy and/or sticky pollen phenotype but resulted in the absence of pollen pigments and pollen that was white, unlike the yellow-colored wild-type pollen and similar to the pollen from *chs* mutants in maize (*Zea mays*) and petunia (*Petunia hybrida*; Coe et al., 1981; Mo et al., 1992; Napoli et al., 1999).

Secondary Screen: Mutant Phenotypes and Gene Isolation

We used auramine O staining and laser scanning confocal microscopy (LSCM) to examine exine in the identified mutants. Exine structure was examined in representatives of different mutant classes that produced mature pollen. While we briefly describe here phenotypes of several primary-screen mutant classes, our further study concentrated primarily on the members of class 1 (glossy and/or sticky pollen) and class 2

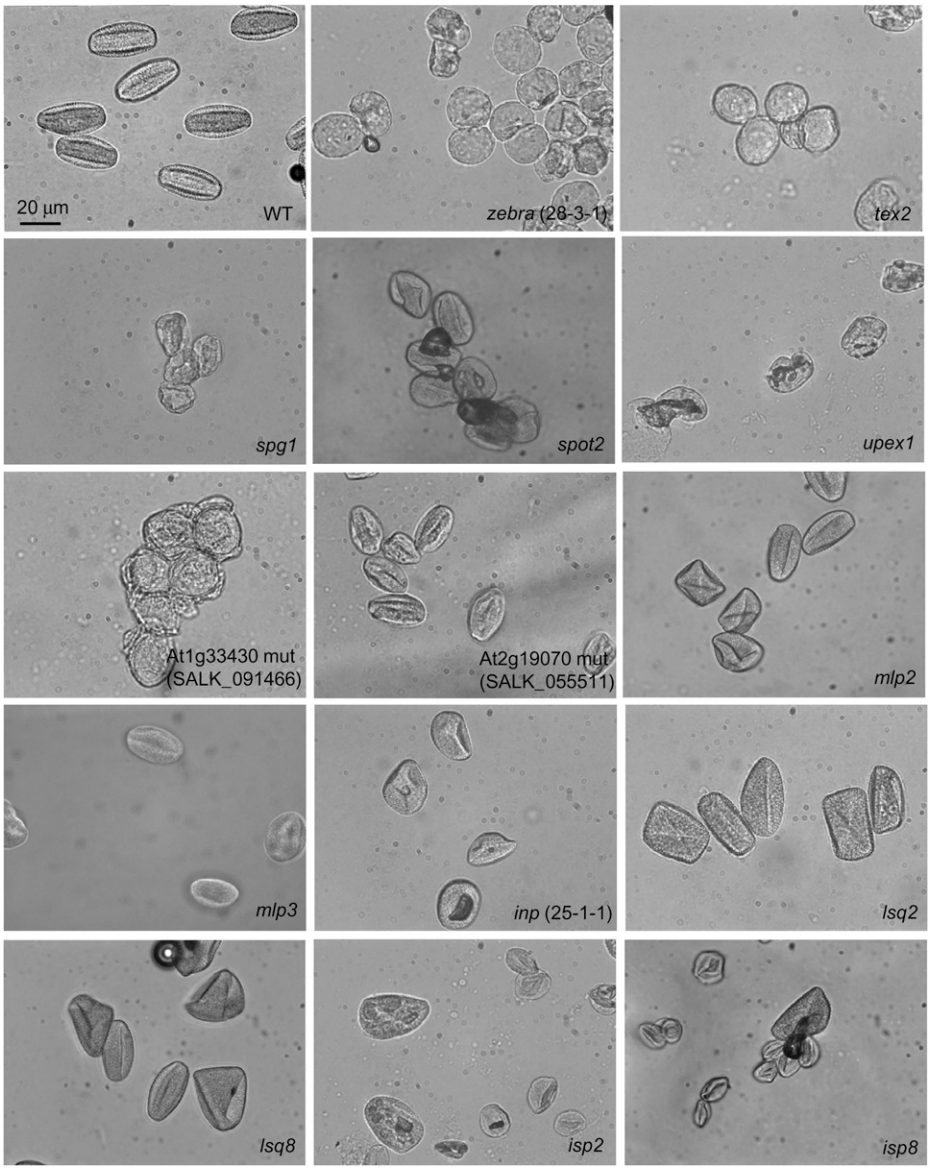

Figure 3. Examples of shape and size distortion in pollen grains observed in the mutants identified in the primary screen. Unhydrated pollen grains were visualized with Zeiss Axioskop. Magnification is the same for all images. WT, Wild type. The mutants shown were assigned to the following primary-screen classes based on their dissecting microscope pollen phenotypes: (1) glossy and/or sticky pollen (*zebra* [28-3-1], *tex2*, *spg1*, *spot2*, *upex1*, SALK_091466 [At1g33430], SALK_055511 [At2g19070], *mlp2*, and *mlp3*); (2) round pollen (*inp* [25-1-1]); (3) large and square pollen (*lsq2* and *lsq8*); (4) irregular-size pollen (*isp2* and *isp8*). Note that more details of pollen morphology are visible in the images obtained with this method than with the dissecting microscopes used for the primary screen. These images, therefore, do not serve to illustrate phenotypic differences used for mutant placement into five classes during the primary screen.

(round pollen), because they exhibited phenotypes more directly related to exine formation. As a result of the secondary screen, 34 mutants from the glossy and/or sticky pollen category, 14 mutants from the round pollen category (*inaperturate* [*inp*]; see below), and one mutant from the little or no pollen category were selected for mapping (Fig. 2).

We used a number of techniques to identify genes responsible for the abnormal exine phenotypes. Because the T-DNA mutagenesis collection was used for the screen, we utilized two different PCR-based methods (McElver et al., 2001; Alonso et al., 2003) to identify positions of the T-DNA insertions. Results of the T-DNA insertion mapping for the lines in which insertions were identified are summarized in Supplemental Table S3. In several cases, the identified T-DNA insertions were responsible for the exine defects. However, in many instances, they did not cosegregate with the observed phenotypes (Dobritsa et al., 2009b; Supplemental Table S3; see below), and for a few lines, we could not identify the positions of the T-DNA insertions. Thus, on a case-by-case basis, we used additional approaches, such as linking the defects to molecular markers through bulked segregant analysis (Michelmore et al., 1991), checking the pollen phenotypes of the sequence-indexed T-DNA insertion lines available for the candidate genes, placing the mutations into complementation groups, comparing the phenotypes of the mutants found in the forward genetic screen with those found through reverse genetics or with previously known exine mutants, followed by PCR amplification and sequencing of these genes in the mutant lines. Table II summarizes the results of the mapping. Below, we describe the secondary-screen exine phenotypes of the mutants and isolation of the affected genes.

Table I. *Genes identified in the reverse genetics screen that, when mutated, affect pollen and anther morphology*

Gene	Primary-Screen Mutant Phenotype	Exine Mutant Phenotype[a]	Annotation/Function	Putative Pathway	Expression Pattern[b]	Insertion Lines Tested
At1g33430	Glossy/sticky pollen	*upex* (allelic to *upex1* and *upex2*)[c]	Glycosyl transferase		Buds (stages 9–12), not in *ap3* and *ag*	SALK_091466
At1g65060	Glossy/sticky pollen	*mlp5*	4-Coumarate-CoA ligase (4CL3)	Phenolics	Buds (stages 9–10), petals	SALK_017894, WiscDsLox503E07
At1g69500	Glossy/sticky pollen	*zebra* (allelic to lines 28-3-1, 37-2-3, 119-1-1, 131-3-1, 155-4-1, 174-154-2)[c]	CYP704B1, fatty acid ω-hydroxylase	Fatty acid	Buds (stages 9–10), not in *ap3* and *ag*	SAIL_1149_B03
At2g19070	Glossy/sticky pollen	*mlp6*	Spermidine hydroxycinnamoyl transferase	Phenolics (spermidine conjugates)	Buds (stages 9–10), not in *ap3* and *ag*	SALK_055511
At3g28780	Glossy/sticky pollen	*mlp7*	Gly-rich protein		Stamen	GT_5_86366
At4g14080	Glossy/sticky pollen	*mlp* (allelic to *mlp4*)[c]	β-1,3-Glucanase/glycosyl hydrolase (A6/MEE48)	Callose degradation	Buds (stages 9–10), not in *ap3* and *ag*	WiscDSLox285F04
At5g13930	White pollen	*mlp8*	Chalcone synthase TT4	Phenolics (flavonoids)	Multiple tissues and stages	SALK_020583

[a]Phenotypic categories developed in the secondary screen with confocal microscopy. For descriptions of the different categories, see "Results." [b]Based on expression data from the microarray (e.g. GENEVESTIGATOR [Zimmerman et al., 2004] and/or Massively Parallel Signature Sequencing [Meyers et al., 2004]) databases. [c]Indicates additional alleles that were found during the forward genetic screen.

Class 1: Glossy and/or Sticky Pollen

This primary-screen class included the largest number of mutants with different abnormalities in the exine structure. Forty-six mutant lines, many of them with dramatic changes in their exines, are described below. These mutants were placed in eight subclasses (secondary-screen categories) based on their exine phenotypes. The number of lines indicated in parentheses below refers to the number of isolates with a particular phenotype that were recovered from different sets of pooled seeds in the forward genetics screen and/or in the reverse genetics screen. Also in parentheses, we indicate the number of established complementation groups (CG) formed by mutants from a given subclass, which suggests the number of affected exine loci.

1A: zebra (Eight Lines/Two CG)

These mutants lacked exine, which was replaced by a thin layer of a material that did not stain well with the exine-specific dye auramine O, and contained rare bits of auramine O-positive aggregates irregularly distributed on the grain surface. We recently described these mutants in detail elsewhere (Dobritsa et al., 2009b). The *zebra* mutants fell into two complementation groups that corresponded to the fatty acid hydroxylase *CYP704B1* and the fatty acyl reductase *MS2* (Dobritsa et al., 2009b).

1B: thin-exine (tex; Four Lines/Three CG)

In these lines, exine was very thin (approximately 0.2–0.4 μm versus 1 μm for the wild-type pollen; Fig. 4). In *tex1*, the reticulate pattern of exine was retained, although large areas of the surface had bare patches where exine was absent. However, in *tex2* to *tex4*, the regular reticulate pattern was no longer present (Fig. 4). Pairwise crosses placed *tex* mutants into three complementation groups composed of *tex1*, *tex2*, and *tex3/tex4*, respectively. Because bulked segregant analysis linked *tex1* to the top of chromosome 1 (Table II) near the exine gene *CYP703A2* (Morant et al., 2007), we sequenced this gene in *tex1* (referred to as line 40-4-1 by Dobritsa et al. (2009b). *tex1* had a single nucleotide change (G to C) in the last exon of *CYP703A2* that caused a Gly-405→Arg conversion. The *tex1* thin-exine phenotype was very similar to that of the *lap4-1* allele (Dobritsa et al., 2009b) of *CYP703A2*. A cross between *tex1* and *lap4-1* demonstrated that they do not complement each other: all 24 F1 progeny had the glossy and sticky pollen phenotype. Thus, *tex1* is an allele of *CYP703A2*.

The *tex2* mutation was linked to the bottom of chromosome 5 (Table II). Additional fine-mapping allowed us to map the mutation to an 82-kb region between 25.926 and 26.008 Mb on chromosome 5. Sequencing of the genes in this interval identified a seven-nucleotide deletion early in the coding region of At5g65000, which encodes a putative nucleotide-sugar transporter (NST). This mutation was termed *tex2-1* and was predicted to lead to protein truncation after the first 29 amino acids. Three insertion lines available for this gene (SALK_001259, SALK_1120886, and CS129638) did not complement the *tex2-1* defects and were referred to as *tex2-2*, *tex2-3*, and *dex2-4*, respectively. *tex2-2* and *tex2-3* had T-DNA insertions in introns 1 and 3, respectively, and *tex2-4* had a transposon inserted in exon 1 at the beginning of the open reading frame (Fig. 5A). All three

Table II. *Mapping of lesions in the mutants with defective exine isolated through the forward genetic screen*

Secondary-Screen Phenotypic Category	Lines Forming a Complementation Group	T-DNA Insertion Site (if Relevant)	Genetic Mapping[a]	Gene Affected/Candidate Gene
zebra	SAIL_1149_B03, 28-3-1, 37-2-3, 119-1-1, 131-3-1, 155-4-1, 174-154-2	SAIL_1149_B03: At1g69500; other lines, various sites	28-3-1 and 37-2-3: bottom of chromosome 1 (markers NGA111 and NGA692)	At1g69500[b-g] (*CYP704B1*), anther-specific fatty acid ω-hydroxylase
zebra	135-2-3		Top of chromosome 3 (markers NGA162 and GAPAB)	At3g11980[b-f] (*MS2*), anther-specific fatty acyl reductase
thin-exine	*tex1*		Top of chromosome 1 (marker F21M12)	At1g01280[c-f] (*CYP703A2*), anther-specific fatty acid in-chain hydroxylase
thin-exine	*tex2*		Bottom of chromosome 5 (markers CIW10 and MBK5)	At5g65000[c-g], NST
thin-exine	*tex3*, *tex4*	*tex4*: At4g35420	*tex3*: NGA1107 marker on chromosome 4; *tex4*: CIW7 marker on chromosome 4	At4g35420[c,e] (*TKPR1/DRL1*), anther-specific tetraketide α-pyrone reductase
spongy	*spg1*		Bottom of chromosome 1 (markers NGA111 and NGA692)	
spongy	*spg2*	At1g27600	Top of chromosome 1 (marker ZFPG)	At1g27600[c,e], putative glycosyl transferase
spongy	*spg3*, *spg4*, *spg5*, *spg6*, *spg7*, *spg8*, *spg9*		*spg3*, *spg4*, *spg7*: chromosome 4 (CIW7 marker)	
spotty	*spot1*	At5g58100		At5g58100[c,f], novel protein
spotty	*spot2*		Top of chromosome 1 (marker F21M12) and bottom of chromosome 5 (markers CIW10 and MBK5)	
spotty	*spot3*, *spot4*		Bottom of chromosome 1 (markers NGA111 and NGA692)	
uneven pattern of exine	*upex1*, *upex2*, SALK_091466	At1g33430		At1g33430[c,f], putative glycosyl transferase, anther specific
uneven pattern of exine	*upex3*		Chromosome 3 (marker GAPAB)	
quartet-defective exine	*qrt-dex1*, *qrt-dex2*	At4g20050		At4g20050[c,f] (*QRT3*), polygalacturonase
defective exine 3	*dex3*		Chromosome 4 (marker CIW7)	
mild or little defects in reticulate pattern	*mlp1*		Chromosome 3 (markers GAPAB, F1P2-TGF, and NGA112)	
mild or little defects in reticulate pattern	*mlp2*	At2g30710		At2g30710[c], RabGAP/TBC domain protein
mild or little defects in reticulate pattern	*mlp3*	At2g30760		At2g30760[c], novel protein
mild or little defects in reticulate pattern	*mlp4*	At4g14080		At4g14080[c,f] (*A6/MEE48*), putative β-1,3-glucanase/glycosyl hydrolase, anther specific

(*Table continues on following page.*)

Table II. (*Continued from previous page.*)

Secondary-Screen Phenotypic Category	Lines Forming a Complementation Group	T-DNA Insertion Site (if Relevant)	Genetic Mapping[a]	Gene Affected/Candidate Gene
inaperturate pollen	25-1-1, 31-1-2, 37-4-1, 41-4-1, 42-4-1, 47-2-1, 52-1-1, 60-4-2, 77-93-1, 83-122-1, 105-1-4, 114/116-3-3, 117-3-7, 118-2-2		25-1-1, 31-1-2, 37-4-1, 52-1-1: chromosome 4 (marker CIW7)	
little or no pollen	*lnp1*		Top of chromosome 3 (marker NGA162)	

[a]Linkage to the indicated markers was established through bulked segregant analysis. [b]For details, see Dobritsa et al. (2009b). [c]Contains a mutation in the gene. [d]Does not complement other mutant alleles of this gene. [e]Bulked segregant analysis demonstrates linkage of the phenotype to the chromosomal region where this gene is located. [f]Other lines with insertions in this gene have identical phenotypes. [g]The mutant phenotype is rescued by a full-size genomic construct.

lines exhibited pollen defects. The first two lines, similar to *tex2-1*, produced fertile plants with glossy and sticky acetolysis-sensitive pollen (Fig. 5C) and the thin-exine phenotype identical to that of *tex2-1* pollen (Fig. 5B). The third line, *tex2-4*, resulted in sterile plants with no pollen produced (Fig. 5D). To confirm the identity of the *TEX2* gene, a complementation construct containing the entire At5g65000 gene under the native promoter was introduced into *tex2-1* and *tex2-4*/+ plants. Wild-type anther and pollen phenotypes were restored in all BASTA-resistant homozygous *tex2-1* (20 lines) and *tex2-4* (seven lines) T1 progeny, confirming At5g65000 as the *TEX2* gene and indicating that the *tex2-4* pollen phenotype and sterility were due to the defects in *TEX2*. Both *tex2-1* and *tex2-4* mutations are located close to each other in the beginning of the coding sequence and are expected to generate null alleles. The reason for the differences in pollen viability and mutant phenotypes between these two alleles is currently unknown. Possibly, the different ecotype backgrounds (Columbia [Col-0] and Landsberg *erecta* [L*er*], respectively) affect the phenotypes of *tex2-1* and *tex2-4*.

Sections of the developing *tex2-4* anthers revealed normal pollen development until stage 9 of anther development (Sanders et al., 1999), when abnormalities were noticed in microspores exhibiting cytoplasm retraction from cell walls (Supplemental Fig. S2). By late stage 11, the *tex2-4* pollen completely degenerated, with cell debris left in the anther locules (Supplemental Fig. S2, E and F). The cytoplasmic shrinkage, such as the one observed in *tex2-4* microspores, is one of the hallmarks of programmed cell death (Buckner et al., 2000; Häcker, 2000) and has previously been described for some mutants with defects in microsporogenesis (Polowick and Sawhney, 1995; Yang et al., 2003; Coimbra et al., 2009), including the *ms1* mutant, in which pollen wall formation is abnormal (Vizcay-Barrena and Wilson, 2006). It could also be caused by plasmolysis (e.g. due to changing osmotic conditions in the locular cavity and compromised cell walls). Interestingly, exine deposition around the developing *tex2-4* microspores was visible in stage 9 anthers (Supplemental Fig. S2C). This was in contrast to the *lap5 lap6* and *acos5* exine mutants, which also demonstrated microspore defects beginning at the same stage and resulted in sterile plants with no mature pollen, but they showed no exine production around the developing microspores (de Azevedo Souza et al., 2009; Dobritsa et al., 2010).

The *tex4* mutant, another member of the thin-exine class, harbored a T-DNA insertion in the last exon of At4g35420, a recently identified tetraketide α-pyrone reductase (*TKPR1/DRL1*; Grienenberger et al., 2010). The importance of the anther-specific *TKPR1/DRL1* for exine production was recently demonstrated (Tang et al., 2009; Grienenberger et al., 2010). The noncomplementing *tex3* mutation mapped to the bottom of chromosome 4 in the vicinity of *TKPR1/DRL1*. However, sequencing of *TKPR1/DRL1* from the *tex3* mutant revealed no nucleotide changes in its coding or noncoding regions, including introns and the 240 bp upstream and 140 bp downstream of the gene. It remains to be seen if *tex3* affects the function of *TKPR1/DRL1*.

1C: spongy (spg; 14 Lines/Three or More CG)

In these mutants, the regular reticulate pattern of exine was not maintained, and on many occasions, instead of a regular net-like structure, exine had irregularly distributed elongated tectum elements and lacunae of variable sizes and shapes, resembling pollen surfaces from the species with rugulate or perforate exine patterns (Fig. 6A). One of the lines (*spg2*) also demonstrated reduced ability to hydrate normally, as many pollen grains in this line retained oval shape upon placement into the aqueous environment (Fig. 6A).

Complementation crosses performed on nine of the *spg* lines placed them into three complementation groups: *spg1*, *spg2*, and *spg3* to *spg9*, respectively. *spg2* harbored a T-DNA insertion in the first intron of At1g27600, a putative glycosyl transferase. Consistent with this, genetic mapping also localized *spg2* to the general vicinity of At1g27600 (Table II). In addition, SALK_037323, a line with an annotated T-DNA insertion at an almost identical position, had the identical pollen exine phenotype. *spg1* was linked to the

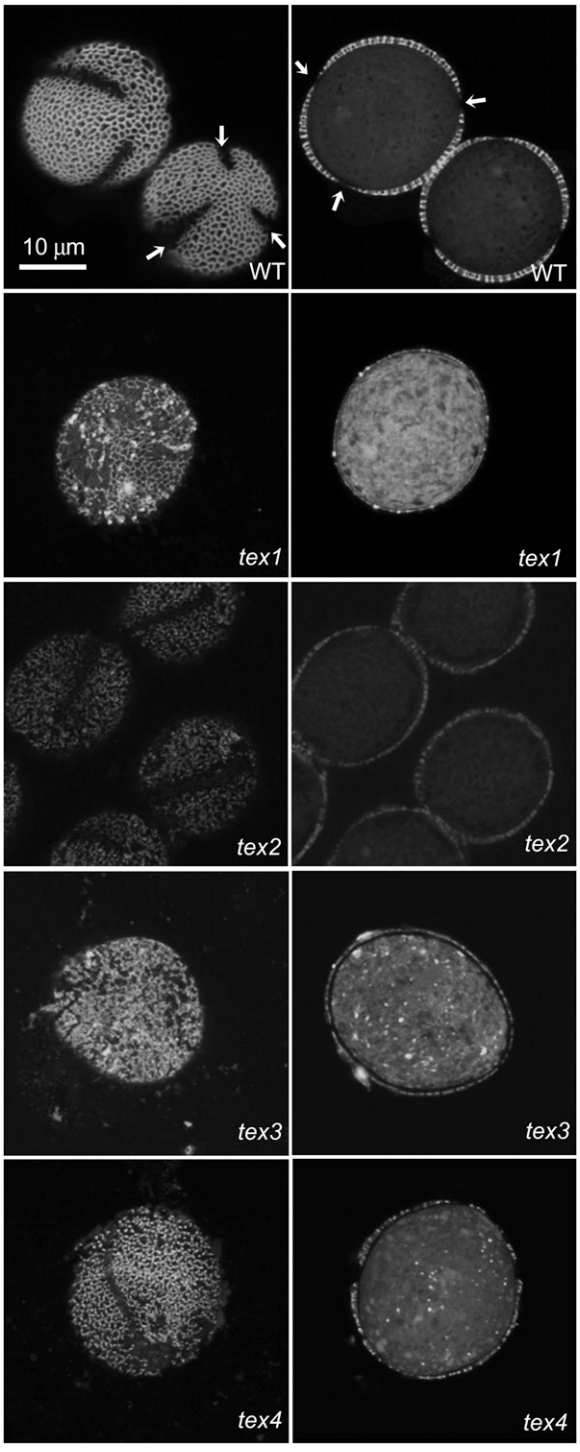

Figure 4. Confocal images of mutant pollen with thin exine. Grains were stained with auramine O. Optical sections through the surface (left) and center (right) of pollen grains demonstrate differences in exine patterns and thickness between the wild type (WT) and four mutants. Magnification is the same for all images. Arrows point to three apertures in the wild-type pollen grains.

markers NGA111 and NGA692 at the bottom of chromosome 1. In the case of the third *spg* complementation group, all three alleles used for mapping (*spg3*/*spg4*/*spg7*) had linkage to the CIW7 marker on chromosome 4.

1D: spotty (spot; Four Lines/Three CG)

In these lines, exine elements appeared to be largely disconnected, indicating possible problems with tectum formation (Fig. 6B).

For *spot1*, both PCR-based methods found an insertion in At5g58100, encoding a novel protein. Three independent sequence-indexed lines (SALK_061320, SALK_041228, and SALK_079847) with T-DNA inserted into different regions of this gene generated plants exhibiting the same pollen exine phenotype, strongly suggesting that mutations in At5g58100 were responsible for the abnormally developed exine.

The rest of the *spot* mutants formed two complementation groups: *spot2* and *spot3/spot4*. For *spot3/spot4*, the defect mapped to the bottom of chromosome 1 (Table II). For *spot2*, surprisingly, linkage to two areas, the top of chromosome 1 (markers F21M12 and ZFPG) and the bottom of chromosome 5 (markers CIW10 and MBK5), was found by bulked segregant analysis. Mapping with additional markers in these regions using 57 individual F2 mutant progeny confirmed this result. We observed a segregation ratio of 208 wild type to 57 mutants for the *spot2* phenotype in F2, consistent with simple Mendelian 3:1 phenotypic segregation ($\chi^2 = 1.64$, $0.5 > P > 0.1$) and with the hypothesis that a single recessive locus was affected. Thus, it remains to be seen what kind of a genomic rearrangement caused this phenotype and this inheritance pattern.

1E: uneven pattern of exine (upex; Four Lines/Two CG)

Three lines (*upex1*–*upex3*) identified through a forward genetics approach had a grossly disorganized exine pattern, with only portions of the pollen surface areas maintaining reticulate structure. *upex1* (Fig. 6C) and *upex2* (data not shown) had very similar types of defects: whereas some surface regions retained reticulate exine, other areas lacked exine or had exine that appeared practically smooth and had small lacunae. In addition, their exine dissociated easily from the pollen surface (Fig. 6C, middle), leaving some grains in the microscopy samples exineless. Another line (SALK_091466) with an identical phenotype was discovered via reverse genetics and had a mutation in At1g33430, a putative glycosyl transferase (Table I). Additional imaging of *upex1* with scanning electron microscopy confirmed the abnormal patterning of exine and the presence of lacunae that were fewer in number and smaller in size than in the wild type (Fig. 7, A–D). Transmission electron microscopy (TEM) of *upex1* pollen demonstrated that its exine had very short baculae and overdeveloped tectum (Fig. 7, E–H). In *upex3*, portions of the surface that were lacking the reticulate exine pattern appeared spotty, giving an im-

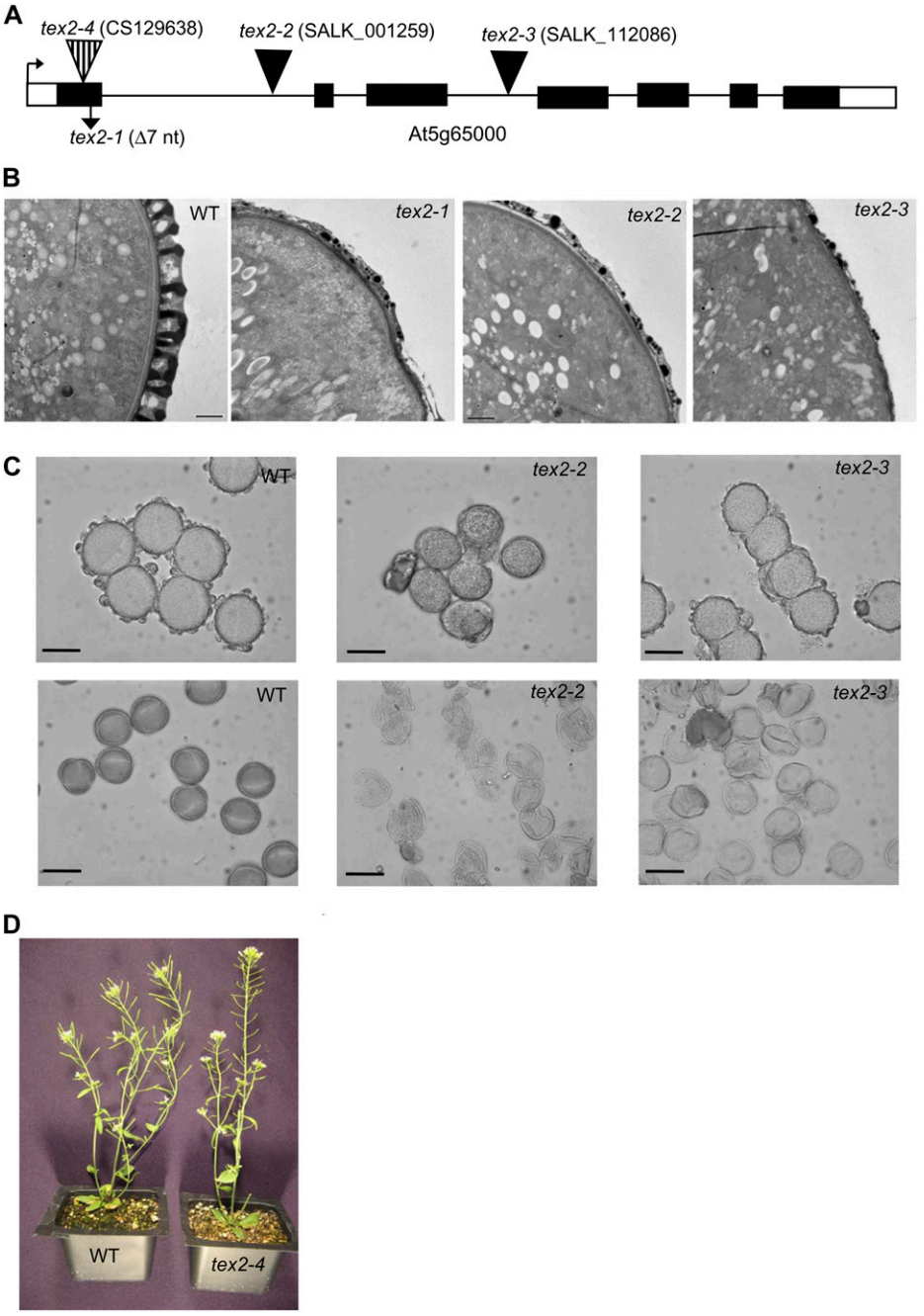

Figure 5. Pollen defects in the *tex2* alleles. A, The At5g65000 gene region. One of the two transcripts supported by the existence of ESTs is shown. Exons are shown as rectangles, with black boxes representing coding regions. Positions of mutations in *tex2-1* to *tex2-4* alleles are shown. The second predicted transcript differs from this one after exon 5 and, therefore, should also be affected in all the mutant alleles. nt, Nucleotides. B, Transmission electron micrographs of pollen grain sections from the wild type (WT), *tex2-1*, *tex2-2*, and *tex2-3*. Exine is abnormally thin in the *tex2* mutants. Bars = 1 μm. C, *tex2* pollen grains are sensitive to acetolysis. Top panels, pollen grains of the wild type, *tex2-2*, and *tex2-3* mock treated with 50 mM Tris-HCl, pH 7.5, have similar morphology. Bottom panels, wild-type pollen grains treated with the acetolysis mixture remain intact, whereas *tex2-2* and *tex2-3* pollen grains are lysed after acetolysis. Bars = 20 μm. D, *tex2-4* plants are sterile and have short siliques compared with the wild type. [See online article for color version of this figure.]

pression that the normal tectum connections were missing between baculae in these areas (Fig. 6C).

The *upex* subclass was composed of three noncomplementing mutants (*upex1*/*upex2*/SALK_091466) and of *upex3*, which complemented the other mutations. For *upex3*, linkage to the GAPAB marker on chromosome 3 was established. The noncomplementing *upex1*/*upex2* lines, as well as SALK_091466, had T-DNA insertions in At1g33430, a putative glycosyl transferase. An unrelated T-DNA insertion in At1g33430 (SAIL_544_C02) had an identical pollen phenotype. According to the public expression databases, such as GENEVESTIGATOR (Zimmermann et al., 2004) and Massively Parallel Signal Sequencing (Meyers et al., 2004), At1g33430 has anther-specific expression in stage 9 to 10 buds (at the time of exine development) and is not expressed in the stamen-lacking *ap3* and *ag* mutants. We confirmed this expression pattern with reverse transcription-PCR and by expressing GUS under the control of the At1g33430 promoter (Supplemental Fig. S3).

1F: quartet-defective exine (qrt-dex; Two Lines/One CG)

Two lines had the glossy and sticky pollen phenotype, which cosegregated with the *qrt* phenotype manifested as defects in microspore separation and

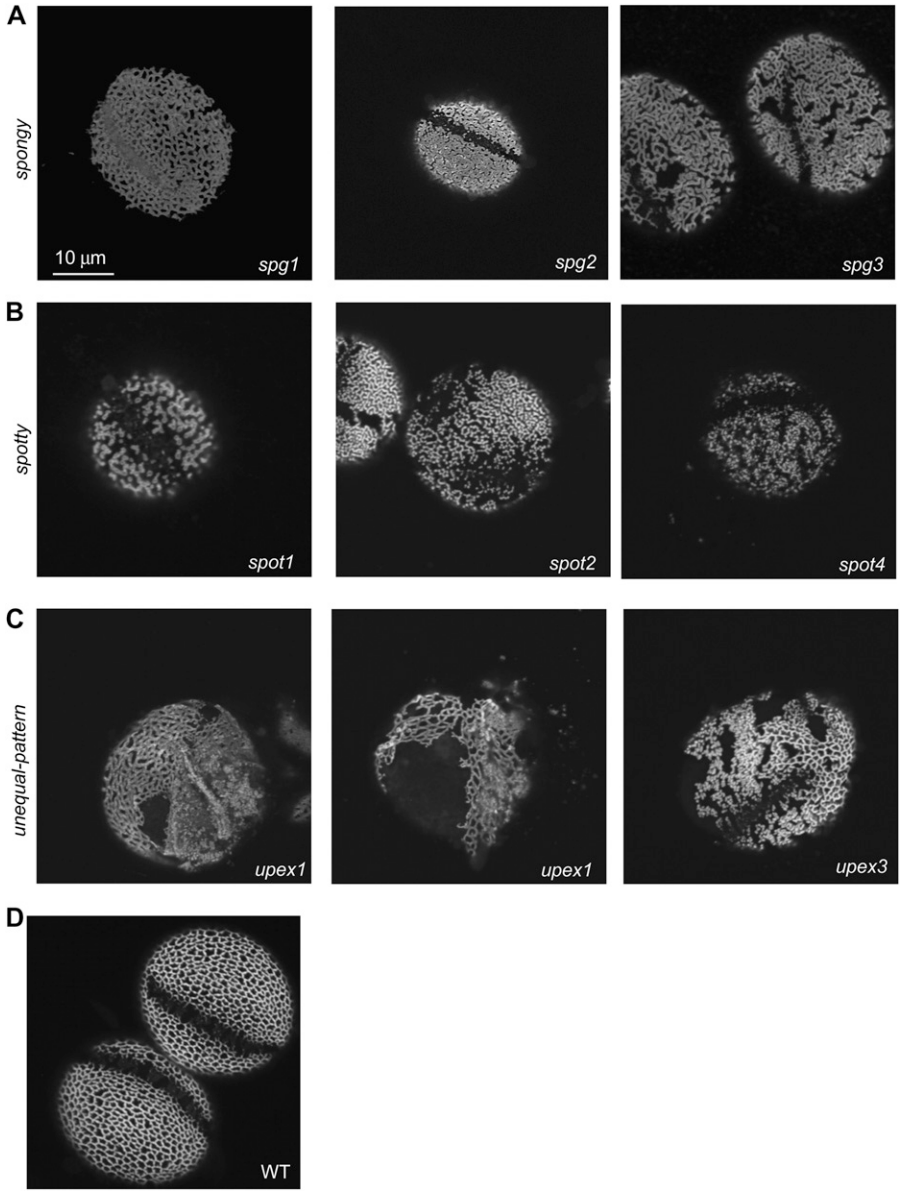

Figure 6. Confocal images of mutant exine surfaces from several subclasses of glossy and/or sticky pollen. A, Examples of mutants with spongy exine. *spg2* has problems with pollen hydration. B, Examples of mutants with spotty exine. C, Lines *upex1* and *upex3* have pollen grains with only portions of exine maintaining reticulate structure. Note the easy shedding of exine in *upex1*. D, The wild type (WT). Grains were stained with auramine O, and magnification is the same for all images.

the resulting release of four products of meiosis as tetrads and not monads of pollen. Pollen exine from these two lines had broader muri and smaller lacunae than the wild type (Fig. 8B; data not shown). Similar exine patterning defects and glossy and sticky pollen phenotypes were previously observed in the mutant alleles of *QRT3* (S. Nishikawa, personal communication). However, these types of exine defects are not generally associated with the *qrt* phenotype, as mutations in the other two *QRT* genes, *QRT1* and *QRT2*, do not cause additional anther- or pollen-associated phenotypes (A.A Dobritsa, unpublished data).

In *qrt-dex1*, a T-DNA insertion was located to the *QRT3* gene. A cross between *qrt-dex1* and *qrt-dex2* did not rescue the mutant phenotypes, indicating that the same gene is likely affected in both lines. QRT3 was previously identified as a polygalacturonase and suggested to degrade the pectic polysaccharides in the primary cell wall of the microspore mother cell (Rhee et al., 2003). Exine phenotypes of *qrt-dex1* and *qrt-dex2* indicate that, in addition to degradation of the primary cell well, polygalacturonase activity is important for proper exine patterning.

1G: defective exine3 (dex3; One or Two Lines)

The original isolate (*dex3-A*) had an abnormal but still largely reticulate exine pattern with irregular aperture margins (Fig. 8C). In the next generation, however, the progeny of this self-fertilized plant segregated phenotypes: whereas some progeny had the parental exine phenotype and normal fertility, the rest of the plants displayed reduced fertility and produced few pollen grains. In the latter case, the pollen grains

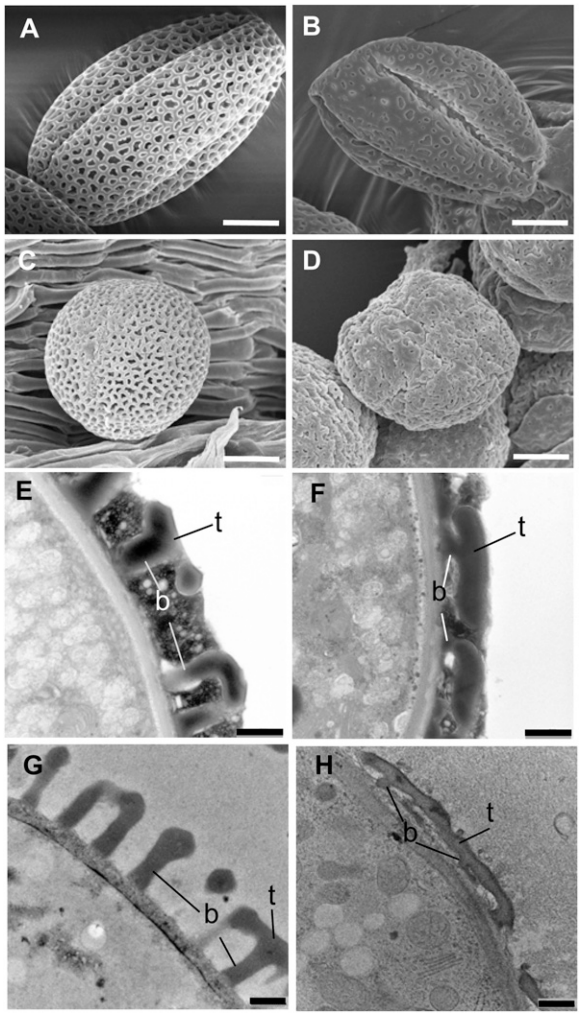

Figure 7. Abnormalities in exine patterning of *upex1* pollen. A to D, Scanning electron micrographs of the surface structure of pollen grains from the wild type (A and C) and the *upex1* mutant (B and D). Samples were prepared without fixation (A and B) or with fixation (C and D). E to H, Transmission electron micrographs of pollen grain sections from the wild type (E and G) and *upex1* (F and H). Note short baculae (b) and overdeveloped tectum (t) of the mutant exine. The TEM images are of the mature pollen (E and F) and of the developing microspores from stage 11 buds (G and H). Bars = 5 μm (A–D) and 500 nm (E–H).

were deformed and had a novel exine phenotype with smaller lacunae and larger surface coverage (*dex3-B*; Fig. 8D).

1H: mild or little defects in reticulate pattern (mlp; Eight Lines/Six or More CG)

Eight mutants had obvious glossy and/or sticky pollen phenotypes when assessed using dissecting microscopes but had few, if any, changes in their exine morphology when visualized using LSCM (Supplemental Fig. S4). In *mlp1*, exine retained the regular reticulate structure but had a finer mesh pattern than the wild-type exine. *mlp2* and *mlp3* had an abnormally shaped glossy pollen (Fig. 3), but their exine had an overall preserved reticulate pattern (Supplemental Fig. S4). Similarly, regular reticulate structure was also present in the glossy pollen of *mlp4* (Supplemental Fig. S4). In addition, four lines identified through reverse genetics (*mlp5–mlp8*, corresponding to At1g65060, At2g19070, At3g28780, and At5g13930, respectively) had very little changes in their exine patterns (Supplemental Fig. S4), despite having glossy and/or sticky pollen phenotypes easily distinguishable at the dissecting microscope level (Supplemental Fig. S1).

Exine is an autofluorescing structure, likely due to the presence of phenolics and, possibly, some other compounds (Roshchina, 2003). To find if exines of the mutants with almost no pattern defects differ from the wild-type exine in their autofluorescence characteristics, we performed LSCM λ scans on pollen surfaces using 405-nm light for excitation. Emission spectra of exines were recorded in the interval of 400 to 625 nm. Under these conditions, the wild-type exine fluorescence spectrum consisted of two peaks: a higher one, with the maximum at 460 nm, and a lower one, at 505 nm (Fig. 9A). To account for individual differences in fluorescence intensity between pollen grains, all the data were normalized to the intensity of the 460-nm peaks. The method generated highly reproducible results: Figure 9A shows three separate trials on the wild-type Col-0 pollen grains (n = 10 grains per trial). When spectra of the mutants were analyzed, we noticed changes in the spectral fingerprints of several

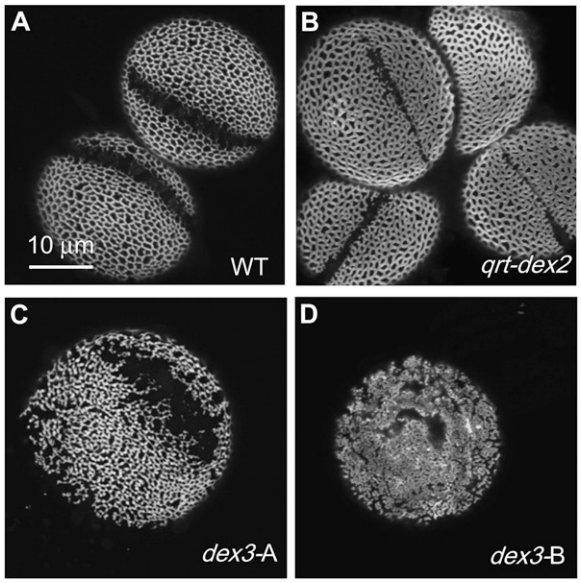

Figure 8. Examples of mutants with *qrt* and *dex3* phenotypes. A, The wild type (WT). B, *qrt-dex2* has a *qrt* phenotype as well as larger exine surface coverage, with broader muri and smaller lacunae. C and D, Two exine phenotypes were observed in the progeny of *dex3*. C, Phenotype of the original isolate (*dex3-A*). D, Novel phenotype segregated in the next generations (*dex3-B*). Grains were stained with auramine O, and magnification is the same for all images.

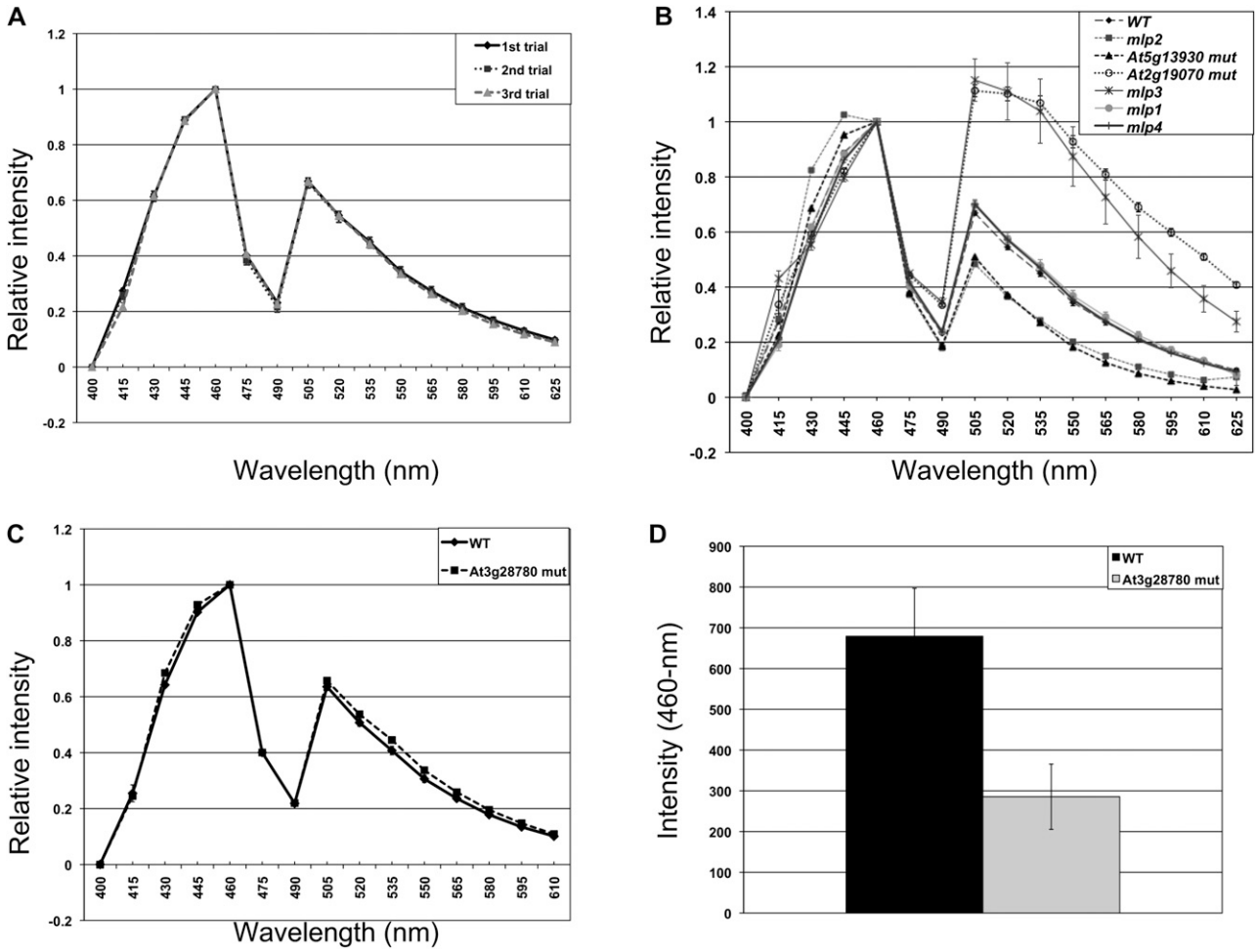

Figure 9. Some mutants with mild or little defects in exine morphology have abnormal exine autofluorescence. Λ scans of exine autofluorescence were recorded in the 400- to 625-nm interval (n = 10 grains per genotype). The data were normalized to 460-nm peak intensity, and means and SE values were calculated. Wild-type exine generates two peaks, the higher one at 460 nm and the lower one at 505 nm. A, The spectra are highly reproducible. Three separate trials were performed on the wild-type exine; n = 10 grains per trial. B, Examples of autofluorescence spectral fingerprints of several mutants. The *mlp1* and *mlp4* lines do not demonstrate noticeable changes in their exine spectra compared with the wild type (WT), while the spectra of the other mutants shown here are significantly different from the wild type. C and D, Although the exine spectrum of the mutant of At3g28780 is not different from the wild type when data are normalized to the 460-nm peaks (C), the absolute fluorescence intensity of the mutant is greatly reduced, demonstrated as intensity of the 460-nm peaks (D).

lines. For instance, both *mlp3* and *mlp6* (At2g19070) showed dramatic increases in the 505-nm peak, which became higher than the 460-nm peak (Fig. 9B). Interestingly, while all the grains in *mlp3* demonstrated a tendency to have a larger 505-nm peak, they exhibited much higher variation in the emission spectra at the longer wavelengths than their wild-type counterparts or other mutants, perhaps reflecting greater differences among the individual *mlp3* pollen in the quantity or quality of materials from which their exine is made. Pollen from *mlp2*, *mlp5* (At1g65060), a different insertion in At1g65060 (WiscDsLox503E07), and *mlp8* (At5g13930) had reductions in the 505-nm peak as well as changes in the shape of the 460-nm peak (Figs. 9B and 10A). For *mlp7* (At3g28780), we detected no changes in the autofluorescence spectrum of exine when the data were normalized to the 460-nm peak (Fig. 9C); however, the absolute fluorescence intensity of the mutant was reduced (illustrated as size of the 460-nm peak in Fig. 9D). Two mutants in this category (*mlp1* and *mlp4*) did not differ from the wild type in their exine fluorescence patterns (Fig. 9B).

For one of the *mlp* mutants, *mlp5*, we also performed TEM analysis of pollen. Interestingly, we found that in TEM images, the mutant exine was consistently less electron dense than the wild-type exine (samples were prepared twice with the same results; trial 1, n = 19 pollen for *mlp5*, n = 14 pollen for the wild type; trial 2, n = 25 pollen for *mlp5*, n = 19 pollen for the wild type [Fig. 10, B and C]). This is

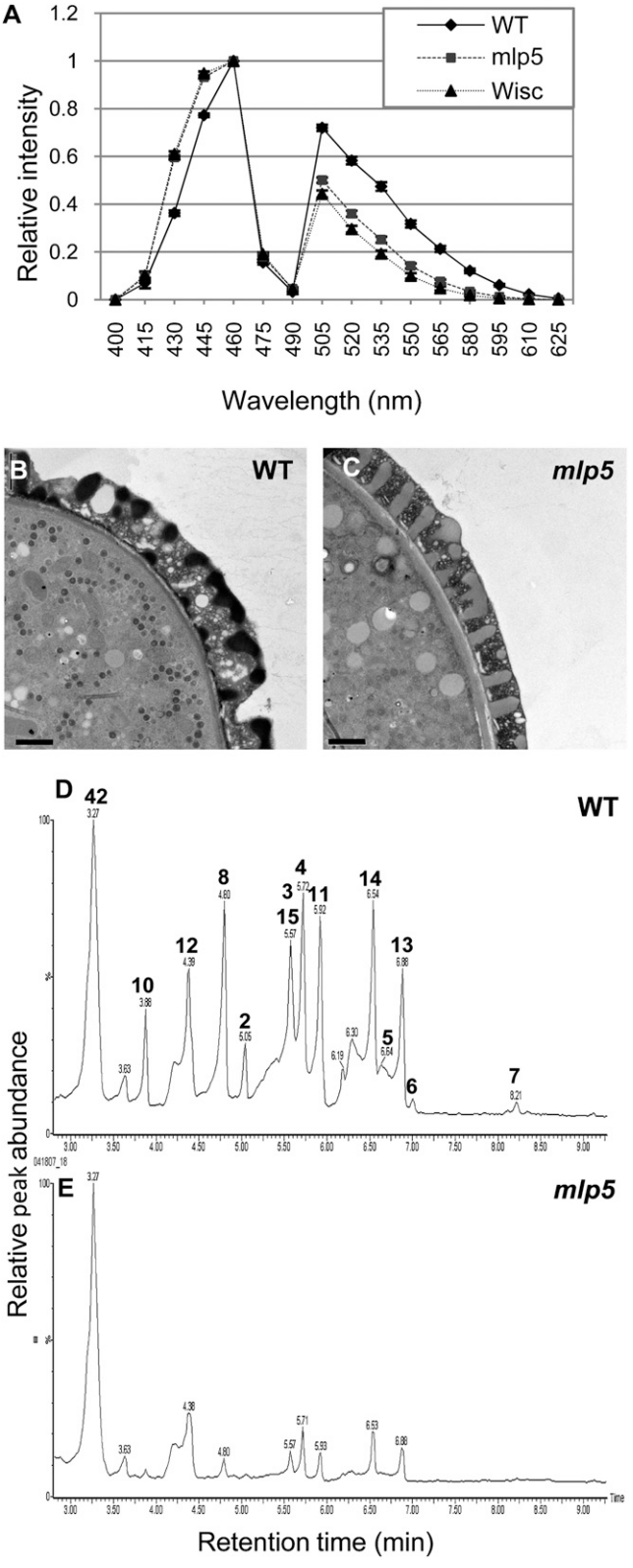

Figure 10. *mlp5* has abnormal pollen exine properties and defects in the production of flavonoids during anther development. A, Exine autofluorescence spectra of the wild-type (WT) and two mutants in the *4CL3* gene (*mlp5* [SALK_017894] and Wisc [WiscDsLox503E07]). B and C, Transmission electron micrographs of pollen grain sections from the wild type (B) and *mlp5* (C). Exine in *mlp5* is less electron dense compared with the wild type. Bars = 1 μm. D and E, Levels of flavonoids produced in stage 9/10 anthers are strongly reduced in *mlp5*. UPLC-quadrupole time-of-flight-MS chromatograms of flavonoids in the wild type (D) and *mlp5* (E) are shown. The peaks in D are annotated in boldface according to the identifier numbers in Supplemental Table S4. Proposed annotations of the peaks are as follows: 2, unknown; 3, kaempherol 7-rhamnoside; 4, kaempherol 3-galactoside-7-rhamnoside; 5, unknown; 6, isorhamnetin 3-glucoside; 7, kaempheride 3-glucoside; 8, quercetin 3-glucoside-7-rhamnoside; 10, unknown; 11, kaempheride 3,7-diglucoside; 12, kaempherol 3-glucoside-7,4′-dirhamnoside; 13, luteolin 4′-methyl ether 7-rutinoside; 14, kaempherol 3-rhamnoside-7-rhamnoside; 15, kaempherol 3-*O*-rutinoside; 42, 8-methylthio-octyl glucosinolate.

consistent with *mlp5* exine having chemical changes that cause it to bind less of the electron-dense stains used in sample preparations.

mlp5 has defects in 4CL3, a 4-coumarate-CoA ligase, which was previously proposed to be involved in one branch of phenylpropanoid metabolism, production of flavonoids (Ehlting et al., 1999). To see what chemical changes *mlp5* exine might have, we performed a metabolomics analysis on extracts from developing (stage 9/10) anthers. Ultra-HPLC coupled to mass spectrometry (UPLC-MS) and gas chromatography-mass spectrometry were used to separate and detect metabolites. The sample preparation and analysis were done as described before (Dobritsa et al., 2010).

Consistent with the proposed role for 4CL3, the most notable change in the metabolic profile of *mlp5*, in comparison with the wild type, was a very strong reduction in the amount of flavonoids (Fig. 10, D and E; Supplemental Table S4). When anther metabolites from *mlp5* and wild-type plants were compared by UPLC-MS, reduction in the levels of multiple glycosides of the flavonoid kaempferol was apparent in the mutant (Supplemental Table S4). Several other kaempherol glycosides (kaempferol 7-rhamnoside, kaempferol 3-galactoside-7-rhamnoside, kaempferide 3-glucoside) were absent in *mlp5*. Additionally, several other flavonoids were missing or had reduced levels, including luteolin 4′-methyl ether 7-rutinoside, quercetin 3-glucoside-7-rhamnoside, and isorhamnetin 3-glucoside (Supplemental Table S4). Associated with the decrease in flavonoids was a concomitant 5-fold increase in Phe, which serves as the entry point into phenylpropanoid pathways (Supplemental Table S5). Interestingly, we also found a 5-fold increase in the amount of another phenolic compound, ferulic acid (Supplemental Table S5), commonly recognized as a precursor in the biosynthesis of the strong plant polymer lignin and suggested to be one of the phenolic precursors of sporopollenin. Based on these results, we hypothesize that changes in exine autofluorescence and TEM staining in *mlp5* may be due to reductions in the amounts of the aromatic constituents of sporopollenin.

Another *mlp* mutant, *mlp4*, harbors a T-DNA insertion in the gene At4g14080, encoding an anther-specific glycosyl hydrolase family 17 protein, A6/MEE48. An

independent transposon insertion into this gene (WiscDSLox285F04) had an identical glossy and sticky pollen phenotype, providing evidence that mutations of the *A6/MEE48* gene are responsible for pollen defects. It has been suggested that A6 is a β-1,3-glucanase that may be important for the dissolution of callose walls around the microspore tetrads (Hird et al., 1993). *mlp2* harbors a T-DNA insertion in At2g30710 that encodes a RabGAP/TBC domain-containing protein, and *mlp3* harbors an insertion in At2g30760 encoding a novel protein. Further studies will be necessary to determine if these genes are in fact required for pollen development. The *mlp1* mutation was localized to chromosome 3 (Table II).

Class 2: Round Pollen (*inp*)

Plants with round pollen and no other pollen/anther defects (e.g. no glossy and/or sticky pollen phenotype) visible at the dissection microscope level were identified among 17 pools of SALK lines and had a very uniform phenotype. The pollen grains of these mutants had a normal reticulate pattern of exine but completely lacked apertures (Fig. 11A) and were dubbed *inp*. Because apertures are often used as exit points for pollen tubes, the fertility of the *inp* plants was assessed. They exhibited well-developed siliques and a normal number of seeds per silique (e.g. 54.2 $\pm$ 3.5 for the *inp* line 25-1-1 versus 51.3 $\pm$ 2.5 for the wild type [n = 12 siliques in both cases]), indicating that pollen tubes in Arabidopsis are capable of breaking through exine walls.

Complementation crosses performed on 14 *inp* lines derived from different seed pools revealed that they all belonged to the same complementation group and, therefore, were most likely allelic. All four of the *inp* lines that were tested with bulked segregant analysis had mutations linked to the CIW7 marker on chromosome 4 (Table II).

Class 3: Little or No Pollen

Mutations in several genes previously implicated in exine production cause the collapse of pollen grains during development, resulting in reduction or complete absence of pollen on dehisced anthers (Aarts et al., 1997; Paxson-Sowders et al., 1997; Wilson et al., 2001; Ito and Shinozaki, 2002; Ariizumi et al., 2004; Dong et al., 2005; Morant et al., 2007; Guan et al., 2008; Tang et al., 2009). In fact, identifying mutants with defects in male fertility was until recently the primary way to discover genes involved in exine development (Aarts et al., 1993; Paxson-Sowders et al., 1997; Ariizumi et al., 2003, 2004; Guan et al., 2008). Thus, during our screen, we have also focused on lines that generated little or no pollen. Approximately 48 such lines were identified. A male-sterile line, *little or no pollen1* (*lnp1*), was found to produce very few glossy pollen grains, which, when examined using LSCM, were found to lack exine (Fig.

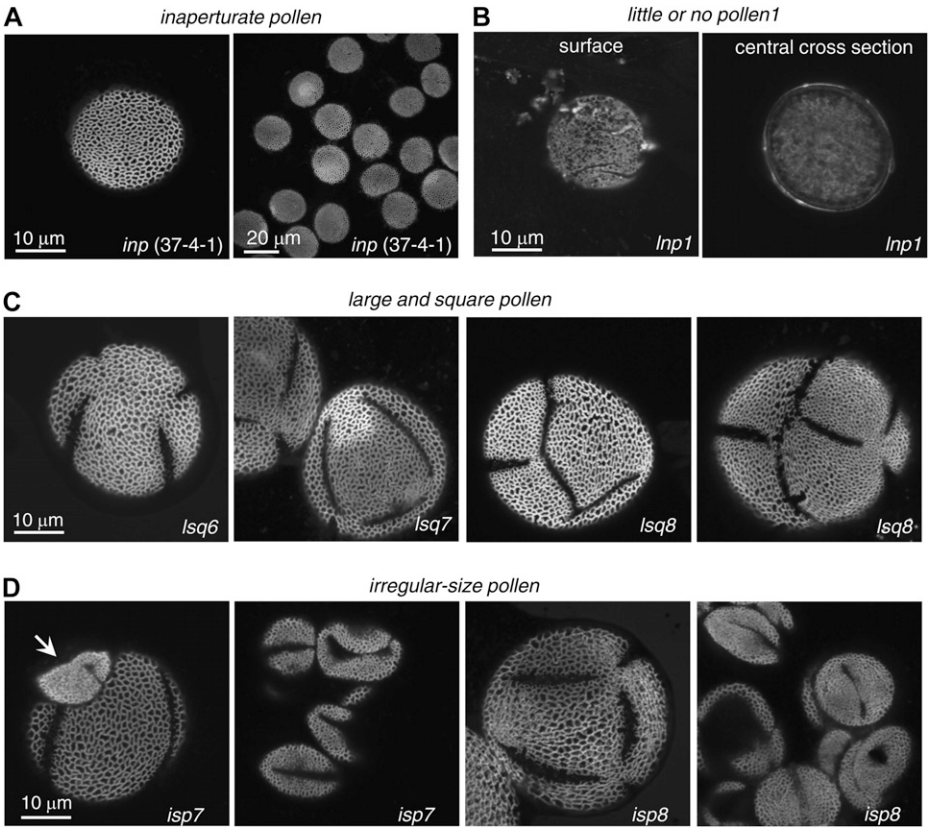

Figure 11. Confocal images of exine from several mutant classes. A, Examples of mutant lines with pollen completely lacking apertures (*inp* phenotype). B, Exine-lacking line *lnp1*, which generates very few pollen grains. C, Examples of mutant pollen that belongs to the large and square pollen (*lsq*) category. Note the abnormal number and positions of apertures. D, Examples of mutant pollen that belong to the irregular-size pollen (*isp*) category. The arrow points to a small grain next to the larger grain (*isp7* [left]); both are derived from the same anther. Larger-than-normal grains sometimes have abnormal number and positions of apertures (*isp8* [left]). Smaller-than-normal grains have smaller lacunae and broader walls, resulting in more excessively covered pollen surface (*isp7*, left and right; *isp8*, right). Grains were stained with auramine O. Magnification is the same as in A (left) for all images except A (right). For reference to the wild-type exine, see Figures 4 and 7.

11B). A mutation in *lnp1* was linked to the marker NGA162 on chromosome 3. Since two known exine genes, *MS2* and *DEX1*, reside in this region, we performed complementation crosses with *ms2* mutants and also PCR amplified and sequenced both genes from the *lnp1* plants. We found that the *lnp1* mutation complemented *ms2*, and the sequences of both *MS2* and *DEX1* genes from this line were indistinguishable from the wild type, indicating that a third gene required for exine production likely resides in this area.

Class 4: Large and Square Pollen

Approximately 30 lines (*large and square pollen1* [*lsq1*]–*lsq30*) were identified. Several lines from this class had pollen with apertures that were abnormal in number or position (Fig. 11C). Grains were significantly larger than those from the wild type. For at least some members of this class (*lsq2*, *lsq3*, and *lsq4*), phenotypes were likely dominant, with F1 plants exhibiting the *lsq* phenotype after a backcross with Col-0. In the F2 generation for these three lines, segregation of three types of progeny was observed: wild-type-looking plants with wild-type pollen; plants with larger flowers and large and square pollen; and finally, dwarf plants with a variety of phenotypic defects, such as bent pistils, anthers with little or no pollen, and sterility. It is known that abnormal meiotic divisions of the microspore mother cells affect the number and placement of apertures in microspores. For instance, when divisions are blocked by colchicine, the whole mother cell acts as a single spherical spore and either does not form apertures or forms one irregular, randomly placed aperture (Sheldon and Dickinson, 1986). Similarly, genetic disruption of male meiotic cytokinesis by mutations in the kinesin-encoding *TETRASPORE/STUD* gene results in the development of large pollen grains with an abnormal number and position of apertures (Hulskamp et al., 1997; Spielman et al., 1997). We hypothesize that similar types of defects may cause the phenotypes that were observed in this class of mutants. This class has not been further pursued.

Class 5: Irregular-Size Pollen

Approximately 36 lines (*irregular-size pollen1* [*isp1*]–*isp36*) were identified. Lines that had this type of defect generated pollen of variable size in the same anther (Fig. 11D; Supplemental Fig. S4). In several cases, the larger than wild-type pollen grains had extra apertures, resembling the *lsq* class of mutants (Fig. 11D; *isp8*). Pollen grains that were smaller than the wild type had exine with a reticulate pattern but smaller than normal lacunae and broader walls or muri, resulting in more excessively covered pollen surface (Fig. 11D). We stained pollen grains in several of those lines with 4′,6-diamino-phenylindole (DAPI) to visualize DNA and discovered that larger grains had two compact generative nuclei and a diffusely stained vegetative nucleus, similar to the wild type (Supplemental Fig. S5). At the same time, all of the smaller grains lacked DAPI staining (Supplemental Fig. S5). Thus, they were not viable pollen but rather empty exine shells, either generated by the disrupted cleavage during meiotic divisions or representing collapsed pollen grains, similar to the ones produced by the mutant defective in the *REVERSIBLY GLYCOSYLATED POLYPEPTIDE* (*RGP1*) and *RGP2* gene functions. Small and collapsed pollen grains in this mutant are products of normal meiotic divisions but later have defects in intine production and pollen mitotic divisions (Drakakaki et al., 2006). This class has not been analyzed further.

DISCUSSION

A Novel Screen Identifies Multiple Pollen Mutants That Have Defective Exine

The field of exine and sporopollenin research, which was at an impasse for a long time, is now at a place similar to where cutin and suberin studies were until a few years ago (for review, see Pollard et al., 2008), when joint chemical, biochemical, and, especially, genetic approaches helped to greatly advance the research in these areas. Whereas the chemical properties of exine's sporopollenin had prevented straightforward characterization of its composition, recent discoveries of several exine genes have reignited interest in this structure and will likely help to gain better understanding of the nature of this unique compound, of the pathways that lead to its production, and of the developmental mechanisms that control exine's assembly into intricate and diverse three-dimensional patterns.

We have conducted a novel genetic screen in Arabidopsis to discover genes involved in pollen exine development. While many of the previously identified genes required for exine development were discovered in screens concentrating on male sterility (van der Veen and Wirtz, 1968; Aarts et al., 1993; Paxson-Sowders et al., 1997; Wilson et al., 2001; Ariizumi et al., 2003, 2004, 2005, 2008; Guan et al., 2008), our studies (Nishikawa et al., 2005; Dobritsa et al., 2009b, 2010) have demonstrated that male sterility or even reduction in male fertility are not the obligate characteristics of mutants with defects in exine-specific genes: many mutants with defects in exine structure have normal fertility. This suggests that male-sterility screens are biased against finding some of the exine mutants. In fact, the results of the screen presented here, as well as the results of the recent *kns* screen that also used a fertility-independent approach (Suzuki et al., 2008), support this notion: most of the mutant lines that we chose for more detailed characterization (53 out of 56) and 11 out of the 12 *kns* mutants have normal fertility, despite sometimes very prominent exine abnormalities. These include, for instance, the *zebra* mutants, in which the exine layer was missing (Dobritsa et al., 2009b).

We used a simple visual screen in which we looked at the state of anthers and pollen grains using standard dissecting microscopes, relying on changes in pollen shape, light reflection, color, and ease of release from anthers to identify potential exine mutants. This method, although labor intensive compared with sterility screens, is nevertheless much simpler than the *kns* screen (Suzuki et al., 2008) performed using scanning electron microscopy or a screen for pollen-stigma adhesion, in which the *lap* mutants affecting exine production were identified (Zinkl and Preuss, 2000; Nishikawa et al., 2005). The strategy proved to be effective: we discovered approximately 213 different mutant lines, which were placed into five phenotypic categories recognized with dissecting microscopes.

A secondary screen among multiple representatives from different categories, which utilized confocal microscopy and concentrated on changes in exine, allowed us to prioritize work with these categories. The glossy and/or sticky pollen category contained mutants with the most striking defects in exine structure and pattern, including those with the zebra, thin-exine, spongy, spotty, uneven-pattern, and defective exine phenotypes, and screening for the glossy and/or sticky pollen phenotype appears to be a reliable way to isolate exine mutants. Most of the mutants (34 identified through the forward screen and six identified through reverse genetics) that we chose to pursue belonged to this category. How could exine abnormalities lead to changes in pollen luster or the tendency of pollen grains to form aggregates? The effects may be direct, caused by changes in the regularity of the net-like tectum or by the aberrant quantity or quality of sporopollenin constituents, which lead to changes in light interaction with the exine surface. Alternatively, they may be indirect, caused, for instance, by changes in the amount of pollen coat that defective exines can hold. This, in turn, may lead to the abnormal light reflection or may mediate clump formation.

The second class of the discovered mutants included those that did not have glossy and/or sticky pollen phenotypes but appeared round using dissecting microscopes. All of these mutants had exines with normal reticulate patterning but lacked apertures.

Finally, because of the negative effect that exine defects have on pollen viability in some mutants (Aarts et al., 1997; Paxson-Sowders et al., 2001; Ariizumi et al., 2004; Guan et al., 2008; de Azevedo Souza et al., 2009; Dobritsa et al., 2009a, 2010), we also kept the lines that produced little or no pollen. Approximately 48 such lines were identified. While only one of these lines (*lnp1*) was pursued here, the rest can be rescreened, looking at the exine formation in these mutants during microspore development.

Disruption of the Exine Gene Network Can Have Many Morphological Outcomes

Mutants discovered in our screen had a variety of exine phenotypes, ranging from very mild (*mlp*) to severe (*zebra*, *tex2*, *lnp1*). Based on the morphology of their exines, we grouped the identified mutants into different subclasses, resulting in *zebra*, *tex*, *spg*, *spot*, *upex*, *qrt-dex*, *dex3*, *mlp*, *inp*, and *lnp* categories. The phenotypic differences in the mutants underscore the fact that exine development is a complex and highly regulated process and that disruption of this process at various points leads to morphological differences in exines.

Although our understanding of the genetic network that facilitates exine synthesis and patterning is still very limited, the identification of some players important for exine development has highlighted the roles of several processes required for exine formation. These include the formation of a temporary callose wall around the pollen mother cell and tetrads of microspores (*CALLOSE SYNTHASE5* gene), primexine deposition (*DEX1*, *NEF1*, *RPG1*), and the production and modification of fatty acid-derived components of sporopollenin (*CYP704B1*, *CYP703A2*, *MS2*, *ACOS5*, *LAP5/PKSB*, *LAP6/PKSA*, *TKPR1/DRL1*, *TKPR2/CCRL6*).

Exine phenotypes of the mutants discovered in our study provide some clues to the roles of corresponding genes. Mutants that have almost no exine or a very thin exine (*zebra*, *tex*) often have defects in genes participating in sporopollenin synthesis or transport. We hypothesize that the currently unknown gene disrupted in *lnp1* may also be involved in this process. The specification of exine reticulate pattern appears to be genetically separate from sporopollenin production, as hypomorphic mutations (*tex1* and *lap4-1*) in a gene involved in sporopollenin biosynthesis (CYP703A2) result in very thin exines, which, nevertheless, have quite regular reticulate patterns.

Phenotypes of some other mutants (*spg*, *spot*, *upex*, *qrt-dex*, *dex3*) suggest that the affected genes are responsible for exine patterning. This process, which in Arabidopsis ultimately results in the development of a regular array of baculae of a certain height and the formation of tectum with regularly distributed lacunae of a certain size, is likely complex. Some of the developmental elements possibly contributing to exine patterning are the formation of primexine of the right thickness and the undulation of plasma membrane at regular intervals: the distribution of membrane protrusions may provide spatial information for the development of future baculae (Takahashi, 1995; Suzuki et al., 2008). At1g33430 disrupted in *upex1* and *upex2* appears to control the height of baculae and the proper fusion of their distal ends to form patterned tectum, and genes affected in *upex3* and the *spot* mutants are likely involved in tectum development. The *spg* mutants resemble the type 3 *kns* mutants (Suzuki et al., 2008), which have incomplete or irregular tectum development. Suzuki et al. (2008) hypothesized that the type 3 *kns* mutants are involved in creating pretectum or in the biosynthesis or deposition of sporopollenin on a growing tectum. We suggest that abnormalities in baculae distribution may also contribute to the phenotypes of the *spg* or type 3 *kns* mutants.

Some of the discovered genes are novel and would have been difficult to identify without a forward genetic screen. For instance, At5g58100 affected in *spot1* encodes a protein with no obvious functional motifs and does not exhibit anther-specific expression. Yet, the existence of three independent lines with insertions in this gene, all exhibiting the same phenotype, indicates that this gene is in fact important for exine development.

Similarly, At5g65000, encoding a putative NST affected in *tex2*, is not anther specific and could be difficult to identify as important for exine development through other approaches. The TEX2 protein is well conserved in the plant kingdom (sharing 73% amino acid sequence identity with orthologs in maize and sorghum [*Sorghum bicolor*], 71% identity with orthologs in rice [*Oryza sativa*] and pine [*Pinus* spp.], and 62% identity with an ortholog in the moss *Physcomitrella patens*). NSTs constitute a family of transmembrane proteins that transport nucleotide-activated sugars from cytoplasm to ER and Golgi lumens, where activated sugars are used as substrates for various glycosyl transferases that synthesize polysaccharides and modify proteins and lipids (Kawakita et al., 1998; Berninsone and Hirschberg, 2000). Although its own substrate specificity is unknown at present, in a multispecies phylogenetic tree of the NST family, TEX2 clusters together with another Arabidopsis protein, At5g41760 (Bakker et al., 2005), capable of transporting CMP-sialic acid into the Golgi apparatus (Bakker et al., 2008). Interestingly, two putative glycosyl transferases (At1g33430/*UPEX1*/*UPEX2* and At1g27600/*SPG2*) were also identified in our screen. It remains to be determined if these proteins depend on TEX2 for their sugar substrates. At1g27600 was recently described as *IRREGULAR XYLEM9-LIKE* and shown to participate as a minor player, along with its closest homolog *IRREGULAR XYLEM9*, in the biosynthesis of the hemicellulose glucuronoxylan, a major component of plant secondary cell walls (Wu et al., 2010). In addition to these enzymes indicating a possible link between carbohydrate metabolism and exine production, the product of the *KNS2* gene, discovered in the *kns* screen, encodes a Suc phosphate synthase (Suzuki et al., 2008). Primexine, the precursor of exine, whose presence is critical for proper sporopollenin deposition and exine formation (Paxson-Sowders et al., 2001; Guan et al., 2008), is made of polysaccharides such as cellulose (Rowley and Dahl, 1977). Therefore, a possibility exists that the NST TEX2, two glycosyl transferases, and the Suc phosphate synthase KNS2 contribute to the synthesis of polysaccharides required for primexine generation.

Mutants with Little Changes in Their Exine Patterns May Have Abnormal Exine Composition

Mutants belonging to one of the subclasses (*mlp*) found in our screen were easily distinguishable as glossy and/or sticky pollen at the dissecting microscope level yet had little, if any, morphological changes in their exine when viewed by confocal microscopy. For some of these mutants, changes in the exine autofluorescence spectrum or in the emission intensity were detected, indicating likely changes in exine composition; for others, no defects were found. Although it is possible that the glossy and/or sticky pollen lines with no apparent changes in exine morphology or fluorescence have defects in the pollen coat rather than in exine per se, to determine if there are some structural changes in the exine of these mutants, other methods may have to be applied. For example, atomic force microscopy can be used to measure the stiffness of the exine material in those mutants. One of those mutants is *mlp4*, affecting the anther-specific *A6* gene. A6 is a glycosyl hydrolase family 17 protein proposed to be important for the timely dissolution of callose walls around tetrads of microspores (Hird et al., 1993). Although the function of A6 has not been formally proven, its expression is strongly correlated with the genes involved in sporopollenin synthesis, such as *ACOS5*, *CYP704B1*, *MS2*, and others. Interestingly, another glycosyl hydrolase family 17 protein (At3g23770) that shares significant homology with A6 has strong coexpression with *A6* and the genes in the predicted sporopollenin biosynthesis network. It is possible, therefore, that A6 and At3g23770 have redundant functions during microspore and exine development and that a double mutant may have more revealing exine phenotypes.

Autofluorescence in plants is often caused by the presence of phenolic compounds, and phenolics in sporopollenin are likely strong contributors to exine autofluorescence. Further studies are necessary to clarify if the *mlp* mutants with abnormalities in the exine autofluorescence spectrum have exine with abnormal phenolic composition. Our study suggested this as a possibility. We found that two *mlp* mutants affecting the flavonoid pathway (*mlp5* and *mlp8*) had pollen exine with lower 550-nm autofluorescence peaks, whereas a mutant affecting the production of hydroxycinnamoyl spermidine (*mlp6*) had a relative increase in the 505-nm peak. At the moment, it is unclear if changes in autofluorescence are caused by changes in these particular phenolic compounds or if they are caused by pleiotropic effects of mutations that affect different metabolites. As more genes required for defined steps in the sporopollenin synthesis pathway are discovered and characterized, their mutants can be used to determine the contribution of the respective components of sporopollenin to exine autofluorescence. It is conceivable that better understanding of exine autofluorescence can lead in the future to novel ways of mutant isolation (e.g. by screening pollen with a fluorescence-activated cell sorter).

For one of the *mlp* lines, *mlp5*, in addition to changes in exine autofluorescence, we also found decreased exine staining in TEM samples. This further supported the notion that although exine patterning was normal in this mutant, its exine composition was altered.

mlp5 has defects in 4CL3, a 4-coumarate-CoA ligase. 4-Coumarate-CoA ligases (EC 6.2.1.12) play roles in

early steps of the phenylpropanoid pathway. They channel carbon flow from primary metabolism to different branches of secondary phenolic metabolism, such as the synthesis of flavonoids or lignin. This process is done by converting 4-coumaric acid and other hydroxycinnamic acids into the corresponding CoA esthers (Hahlbrock and Scheel, 1989; Douglas, 1996). Based on the in vitro properties of the enzyme, its expression patterns, and evolutionary relationships, it has been suggested that 4CL3 in Arabidopsis is likely involved in flavonoid metabolism and not in the production of lignin or other phenolic compounds (Ehlting et al., 1999). Consistent with the involvement of 4CL3 in flavonoid production, our metabolite profiling analysis of the extracts from developing *mlp5* anthers at the time of exine production revealed a dramatic reduction in the amount of flavonoids. Additionally, we found a 5-fold increase in the accumulation of Phe, a precursor of phenolic compounds, and, interestingly, a similar 5-fold increase in the accumulation of ferulic acid, which is known as a precursor in lignin production. Previously, the in vitro studies of 4CL3 enzymatic activities demonstrated that although the enzyme had the strongest substrate specificity toward 4-coumarate, it also possessed a noticeable activity toward ferulate (Ehlting et al., 1999; Costa et al., 2005). Results of chemical analyses of sporopollenin suggested that both ferulic and 4-coumaric acids are possible constituents of sporopollenin (Schulze Osthoff and Wiermann, 1987; Wehling et al., 1989; Rozema et al., 2001; de Leeuw et al., 2006). Based on our results, we hypothesize that among the roles of 4CL3 in anthers may be the synthesis of phenolic components of sporopollenin and that ferulate-CoA and 4-coumarate-CoA may either be directly incorporated in sporopollenin or act as precursors for sporopollenin's phenolic components. At present, it is unknown if a reduction in the amount of flavonoids in *mlp5* anthers indicates that they are also used as precursors in sporopollenin synthesis or, more likely, reflects 4CL3 participation in another pathway (e.g. the production of flavonoids for pollen coat). The 4CL3 products may also contribute to the recently discovered pathway leading to the formation of hydroxycinnamoyl spermidines in pollen (Fellenberg et al., 2008, 2009; Grienenberger et al., 2009; Matsuno et al., 2009). These spermidine conjugates are components of pollen coat (Grienenberger et al., 2009), yet there is some evidence that they may also be present in exines (Gubatz et al., 1986).

Aperture Development in Exines Is Specified Separately from the Reticulate Pattern

The round pollen category contained mutants with pollen entirely lacking apertures (*inp* phenotype) but with a normal reticulate pattern, indicating that these types of exine elements are specified separately. All 14 *inp* lines that were tested for complementation were noncomplementing, suggesting that these mutations were allelic. Identification of the mutants with inaperturate pollen raises interesting developmental and evolutionary questions. In pollen of most plant species, apertures represent a well-defined and tightly controlled element of exine patterning, and they are species specific in number and morphology. This indicates that the exine deposition machinery reliably recognizes some areas on the pollen surface as different from others and does not deposit exine into these areas. How pollen generates and defines these functionally distinct cellular domains and then translates cellular asymmetries into extracellular differences is an exciting developmental and cell biological problem. The product of the *INP* gene is likely involved either in asymmetry establishment or in its interpretation. Given the variety of aperture morphologies across the phylogenetic spectrum of plants, understanding of the cellular mechanism for generating extracellular asymmetries will eventually allow investigation of the evolutionary malleability of these types of programs in a well-defined system that provides an enormous diversity of structures to probe.

In Arabidopsis, apertures are formed at the points of contact between neighboring microspores in a tetrahedral tetrad generated through simultaneous microsporogenesis (Owen and Makaroff, 1995; Furness and Rudall, 2004). It would be interesting to see if the shape of microspore tetrads and their development in *inp* mutants (e.g. simultaneous versus successive microsporogenesis) differ from those of the wild type. It was demonstrated in other plant species that proper aperture positioning is microtubule dependent (Dover, 1972; Sheldon and Dickinson, 1983, 1986). Also, the formation of an ER shield (the colpal shield), which blocks the deposition of primexine and sporopollenin at the sites of future apertures, was suggested to account for the development of apertures, at least in some species (Heslop-Harrison, 1963, 1968b). It would be important to check if microtubule formation, meiotic spindle orientation, and ER positioning are normal in these mutants. Identifying the gene defective in this complementation group will likely provide additional information about the mechanism that determines the number and positions of apertures.

The *inp* mutants are also ideal for addressing the functional roles of apertures. Traditionally, apertures have been regarded as points of exit for germinating pollen tubes. In fact, for pollen tubes of many plant species for which detailed studies of pollen germination have been performed, apertures are the only way out (Heslop-Harrison, 1979b; Cresti et al., 1985; Heslop-Harrison and Heslop-Harrison, 1985, 1992). However, in Arabidopsis, pollen tubes do not always use apertures and often break out through the exine walls (Edlund et al., 2004). Additionally, inaperturate pollen, although much less common, does exist among all major plant groups (many gymnosperms, some monocots [e.g. members of Orchidaceae, Liliaceae, and Zingiberaceae], and a few eudicots [e.g. some taxa in Solanaceae, Salicaceae, and Ranuncula-

ceae]) and has independently evolved numerous times (Furness, 2007). Most members of the Brassicaceae family, to which Arabidopsis belongs, have fairly uniformly patterned pollen with reticulate exine and three slit-like apertures (Rollins and Banerjee, 1979). However, examples of plants with inaperturate pollen also exist in Brassicaceae (e.g. *Matthiola incana* has spheroidal pollen with reticulate exine and no apertures; Furness, 2007). It has been suggested that the evolution of pollen with apertures of the type that Arabidopsis possesses (tricolpate pollen), which is very widespread among eudicots, is a potential key innovation ensuring selective advantage and underlying eudicot success (Furness and Rudall, 2004). Our recovery of the *inp* mutants in Arabidopsis will provide a means to test this hypothesis. The *inp* mutants displayed apparently normal fertility. Careful in vitro and in vivo studies of pollen germination, as well as competitive crosses using wild-type and inaperturate pollen, will be required to determine if having three apertures gives pollen a significant advantage in germination.

Difficulties in the Isolation of Exine Genes Found through Forward Genetic Screening of the SALK Collection

We chose to screen the T-DNA-mutagenized SALK collection (Alonso et al., 2003) with a goal of fast recovery of the mutated sequences that cause defective exine phenotypes. However, we found that for a significant number of mutants that were pursued, mutations causing abnormal exine phenotypes were not directly associated with T-DNA insertions (Table II; Supplemental Table S3). This made the isolation of the responsible genes far from straightforward. For example, for all seven *zebra* isolates identified in the forward screen, the T-DNA insertions were not localized to the genes later found to be responsible for the exine phenotypes (*CYP704B1* and *MS2*). When the nature of the mutations was finally determined for the *zebra* lines, we found examples of short deletions (one and 42 nucleotides long), a larger genomic rearrangement, and single-nucleotide substitutions (Dobritsa et al., 2009b). Similarly, for the thin-exine lines *tex1* and *tex2*, the T-DNAs were mapped to positions completely different from the ones found to be responsible for the mutant phenotypes, and the mutations causing the phenotypes were identified as a single-nucleotide substitution and a seven-nucleotide deletion, respectively. In addition, for *tex3*, *spg5*, *upex2*, *lnp1*, and the four lines belonging to the *inp* complementation group, the T-DNA insertions were mapped to chromosomes different from the one to which the mutations were linked through bulked segregation analysis. In *spot2*, bulked segregation analysis linked the defect to the regions of both chromosomes 1 and 5, indicating the possibility of a translocation or another genomic rearrangement.

T-DNA or transposon integrations in Arabidopsis have been previously associated with chromosomal rearrangements, large and small deletions, and translocations (Forsbach et al., 2003; Boavida et al., 2009), and examples of the recovery of point mutations through T-DNA screens have been described (Dieterle et al., 2001; Takeda et al., 2004; Marrocco et al., 2006). Yet, the frequency of such events in our collection of isolates appears to be quite high, making the SALK collection less attractive for use in forward genetic screens than we expected. These features might be more common than is usually anticipated for T-DNA-mutagenized collections, because a recent forward genetic screen of the T-DNA Versailles collection followed by the mapping of the recovered mutations revealed a very similar trend in terms of a high number of non-T-DNA-tagged mutated genes that instead displayed single-nucleotide changes, small deletions, and other genomic rearrangements (De Muyt et al., 2009).

MATERIALS AND METHODS

Forward Genetic Screen

We screened pooled T-DNA insertion lines derived from the SALK collection (Alonso et al., 2003). The Col-0 ecotype of Arabidopsis (*Arabidopsis thaliana*) served as the wild-type control. The entire content of each vial containing pooled T3 and T4 seeds from 100 individual lines was planted onto four flats on a 1:1 mix of C2 (Conrad Fafard) and Metro-Mix (Sun Gro Horticulture) or Schultz Potting Soil Plus (Spectrum Brands) soil. Plants from 179 seed pools were screened (individual sets of pools CS75001–CS75003, CS75007, and CS75011–CS75185 from the combined sets of pools CS76502 and CS76504 were obtained from the Arabidopsis Biological Resource Center [ABRC]). Plants were grown either in a greenhouse (in an air-conditioned room at 22°C) under ambient light conditions or in growth chambers with 12 h of 100 μE m^{-2} s^{-1} fluorescent lighting at 22°C. Six hundred to 800 plants were grown and screened from most vials, and we considered this an equivalent of screening approximately 100 individual lines. Zeiss Stemi-2000C, Olympus SZ51, or equivalent dissecting stereomicroscopes with magnification of 50× to 80× were used. Open flowers were collected, pollen was brushed on a microscope slide, and anthers were examined for abnormalities in anther or pollen morphology. Neither anthers nor pollen underwent any treatment for primary screening. More than 123,000 plants were screened. We estimate that we screened an equivalent of at least 16,000 individual lines. Mutants with potential exine defects were backcrossed with Col-0 at least once.

Reverse Genetic Screen

Available insertion mutants for 49 candidate exine genes were obtained from the ABRC or the Nottingham Arabidopsis Stock Center. One or two insertion lines were used for each gene, with a preference given to those with insertion positions within predicted protein-coding regions. Thirty-six plants were grown for each line. We confirmed the presence of insertions in the lines using gene-specific primers developed through the SIGnAL iSect Primer Design program (http://signal.salk.edu/isects.html). For a list of primers used to confirm insertions, see Supplemental Table S6. Screening methods were identical to those used for the forward genetic screen. Once potential exine mutants were identified, their phenotypes were confirmed in the next generation, and plants were backcrossed with a background ecotype (Col-0 or L*er*) at least once.

Phenotypic Analysis during the Secondary Screen

Shapes of unhydrated pollen were assessed by placing pollen grains in 100% glycerol and examining with a 100× objective on a Zeiss Axioskop compound microscope (Nomarski optics). To visualize the exine structure, pollen grains were removed from anthers onto a microscope slide (by gently brushing an anther on a slide or by removing pollen with thin forceps), and a small drop of auramine O solution was added to pollen. Auramine O was

dissolved in 50 mM Tris-HCl, pH 7.5, and diluted to 0.001% in 17% Suc. Pollen grains were simultaneously hydrated and stained with auramine O and then examined with a laser scanning confocal microscope (Olympus Fluoview FV1000, 100× objective, fluorescein isothiocyanate settings). In addition to images of the exine surface, we took optical sections by LSCM through the center of pollen grains to determine exine thickness. Multiple pollen grains were observed for each line ($n \geq 20$). For lines exhibiting interesting abnormal exine phenotypes, pollen from multiple flowers (and multiple plants, after the lines were established) was assessed. For most mutant lines, the phenotypes of all grains in each line were very similar. The exceptions to this were *lsq* and *isp* lines, which produced pollen of different sizes, shapes, or aperture placement, progeny of the *dex3* isolate, which segregated two different mutant exine phenotypes, and *upex* lines, in which all pollen grains had abnormal exine yet particular patterning defects and the placement of reticulate patches varied from grain to grain. Scanning electron microscopy, TEM, and acetolysis were performed as described (Dobritsa et al., 2009b). Sectioning of developing anthers and toluidine blue staining were performed as described (Dobritsa et al., 2010).

Spectral Analysis of Exine Autofluorescence

Pollen grains were mounted in 100% glycerol, illuminated using a 405-nm laser (14% laser power), and adjusted for focus and photomultiplier tube voltage using AlexaFluor488 settings. Lambda scans were performed on exine surfaces ($n \geq 10$ grains) using a laser scanning confocal microscope (Olympus Fluoview FV1000, 100× objective, scan interval of 400–625 nm, step size of 15 nm, bandwidth of 15 nm). Background intensity was subtracted, then intensity data were normalized to the intensity of the 460-nm peaks and mean and SE values were calculated.

Identification of Exine Genes

Two PCR methods were used to map T-DNA insertions in the lines discovered via forward screen: the adapter-based method used by Alonso et al. (2003) for mapping positions of SALK T-DNA insertions, and thermal asymmetric interlaced-PCR (McElver et al., 2001). Whenever possible, after determining the positions of T-DNA insertions, we confirmed that the disrupted gene was responsible for the observed phenotype by checking the phenotypes of additional insertion alleles available from the ABRC. For lines with causal mutations unlinked to the T-DNA, we crossed the lines with defective exine with the L*er* ecotype and performed bulked segregant analysis to identify the genomic intervals in which the mutations were located. We used five to six molecular markers per chromosome available through The Arabidopsis Information Resource (http://www.arabidopsis.org/). Complementation crosses were performed on mutants with similar exine phenotypes. In several cases, we identified an affected gene by comparing exine phenotypes of the mutants isolated via the forward genetic screen with mutants identified through reverse genetics, performing complementation analysis, and sequencing the gene. To complement the *tex2* defects, the At5g65000 gene (from 516 nucleotides upstream of the start codon to 251 nucleotides downstream of the stop codon) was amplified by PCR (primers *Sac*I-At5g65000-FF [5′-GAGCTCTTCAACCCGAGGACATGAGAAG-3′] and *Age*I-At5g65000-IR [5′-ACCGGTATTCAAAACTGTATACATCATGTG-3′]), digested with *Sac*I/*Age*I, and introduced into the modified binary vector pGreenII02229 (Hellens et al., 2000; von Besser et al., 2006). Homozygous *tex2-1* and heterozygous *tex2-4*/+ plants were transformed by the floral dip method (Clough and Bent, 1998), and transgenic plants were selected with BASTA. Homozygous *tex2-4* progeny were identified among the transgenic T1 plants using a diagnostic PCR (primers CS129638-LP [5′-TTGTAACTCGATCCACCCTTG-3′], CS129638-RP [5′-GATAACGCGAAAGGTTACACG-3′], and DS3-1 [5′-ACCCGACCGGATCGTATCGGT-3′]).

The Arabidopsis Genome Initiative locus numbers for the genes analyzed in this article are as follows: *CYP703A2* (At1g01280), At1g27600, At1g33430, *4CL3* (At1g65060), *CYP704B1* (At1g69500), *SHT* (At2g19070), *MS2* (At3g11980), At3g28780, *A6/MEE48* (At4g14080), *QRT3* (At4g20050), *TKPR1/DRL1* (At4g35420), *TT4* (At5g13930), At5g58100, At5g65000.

Supplemental Data

The following materials are available in the online version of this article.

Supplemental Figure S1. Examples of anthers from mutants that have the glossy and/or sticky pollen phenotype.

Supplemental Figure S2. Microspores produced by the *tex2-4* mutant degenerate during development.

Supplemental Figure S3. At1g33430 is expressed in the developing anthers.

Supplemental Figure S4. Examples of glossy and/or sticky pollen mutants that exhibit a normal reticulate pattern under LSCM.

Supplemental Figure S5. DAPI staining of irregular-size pollen (*isp*).

Supplemental Table S1. Candidate genes that did not affect pollen and anther morphology, when mutated.

Supplemental Table S2. Candidate genes in which the analysis did not produce conclusive results.

Supplemental Table S3. Positions of the T-DNA insertions mapped for various mutants identified in the screen.

Supplemental Table S4. UPLC-MS analysis of metabolite levels in the extracts from wild-type and *mlp5* developing anthers.

Supplemental Table S5. Gas chromatography-mass spectrometry analysis of metabolite levels in the extracts from wild-type and *mlp5* developing anthers.

Supplemental Table S6. Primers used to verify the positions of T-DNA insertions in candidate genes.

ACKNOWLEDGMENTS

We thank undergraduates Veder Garcia, Carol Casey, Gatoya Jones, Alex Hoover, Andrew Mutka, and Jacob Roshanmanesh for help with the forward genetic screen and bulked segregant analysis, Jean Greenberg and Aretha Fiebig for critical reading of the manuscript, the ABRC and the Nottingham Arabidopsis Stock Center for mutant resources, and John Zdenek, Judy Coswell, and Sandra Suwanski at the University of Chicago greenhouse for excellent plant growth facilities.

Received May 4, 2011; accepted August 15, 2011; published August 17, 2011.

LITERATURE CITED

Aarts MG, Dirkse WG, Stiekema WJ, Pereira A (1993) Transposon tagging of a male sterility gene in Arabidopsis. Nature **363:** 715–717

Aarts MG, Hodge R, Kalantidis K, Florack D, Wilson ZA, Mulligan BJ, Stiekema WJ, Scott R, Pereira A (1997) The Arabidopsis MALE STERILITY 2 protein shares similarity with reductases in elongation/condensation complexes. Plant J **12:** 615–623

Ahlers F, Bubert H, Steuernagel S, Wiermann R (2000) The nature of oxygen in sporopollenin from the pollen of *Typha angustifolia* L. Z Naturforsch C **55:** 129–136

Ahlers F, Thom L, Lambert J, Kuckuk R, Wiermann R (1999) ^{1}H NMR analysis of sporopollenin from *Typha angustifolia*. Phytochemistry **5:** 1095–1098

Alonso JM, Stepanova AN, Leisse TJ, Kim CJ, Chen H, Shinn P, Stevenson DK, Zimmerman J, Barajas P, Cheuk R, et al (2003) Genome-wide insertional mutagenesis of *Arabidopsis thaliana*. Science **301:** 653–657

Ariizumi T, Hatakeyama K, Hinata K, Inatsugi R, Nishida I, Sato S, Kato T, Tabata S, Toriyama K (2004) Disruption of the novel plant protein NEF1 affects lipid accumulation in the plastids of the tapetum and exine formation of pollen, resulting in male sterility in Arabidopsis thaliana. Plant J **39:** 170–181

Ariizumi T, Hatakeyama K, Hinata K, Sato S, Kato T, Tabata S, Toriyama K (2003) A novel male-sterile mutant of *Arabidopsis thaliana, faceless pollen-1*, produces pollen with a smooth surface and an acetolysis-sensitive exine. Plant Mol Biol **53:** 107–116

Ariizumi T, Hatakeyama K, Hinata K, Sato S, Kato T, Tabata S, Toriyama K (2005) The *HKM* gene, which is identical to the *MS1* gene of *Arabidopsis thaliana*, is essential for primexine formation and exine pattern formation. Sex Plant Reprod **18:** 1–7

Ariizumi T, Kawanabe T, Hatakeyama K, Sato S, Kato T, Tabata S, Toriyama K (2008) Ultrastructural characterization of exine develop-

ment of the *transient defective exine 1* mutant suggests the existence of a factor involved in constructing reticulate exine architecture from sporopollenin aggregates. Plant Cell Physiol **49:** 58–67

Bakker H, Routier F, Ashikov A, Neumann D, Bosch D, Gerardy-Schahn R (2008) A CMP-sialic acid transporter cloned from *Arabidopsis thaliana*. Carbohydr Res **343:** 2148–2152

Bakker H, Routier F, Oelmann S, Jordi W, Lommen A, Gerardy-Schahn R, Bosch D (2005) Molecular cloning of two Arabidopsis UDP-galactose transporters by complementation of a deficient Chinese hamster ovary cell line. Glycobiology **15:** 193–201

Berninsone PM, Hirschberg CB (2000) Nucleotide sugar transporters of the Golgi apparatus. Curr Opin Struct Biol **10:** 542–547

Blackmore S, Barnes SH (1986) Harmomegathic mechanisms in pollen grains. *In* S Blackmore, IK Ferguson, eds, Pollen and Spores: Form and Function, Vol 12. Academic Press, London, pp 137–149

Boavida LC, Shuai B, Yu H-J, Pagnussat GC, Sundaresan V, McCormick S (2009) A collection of Ds insertional mutants associated with defects in male gametophyte development and function in Arabidopsis thaliana. Genetics **181:** 1369–1385

Buckner B, Johal GS, Janick-Buckner D (2000) Cell death in maize. Physiol Plant **108:** 231–239

Clough SJ, Bent AF (1998) Floral dip: a simplified method for Agrobacterium-mediated transformation of *Arabidopsis thaliana*. Plant J **16:** 735–743

Coe EH, McCormick SM, Modena SA (1981) White pollen in maize. J Hered **72:** 318–320

Coimbra S, Costa M, Jones B, Mendes MA, Pereira LG (2009) Pollen grain development is compromised in Arabidopsis *agp6 agp11* null mutants. J Exp Bot **60:** 3133–3142

Costa MA, Bedgar DL, Moinuddin SGA, Kim K-W, Cardenas CL, Cochrane FC, Shockey JM, Helms GL, Amakura Y, Takahashi H, et al (2005) Characterization in vitro and in vivo of the putative multigene 4-coumarate:CoA ligase network in Arabidopsis: syringyl lignin and sinapate/sinapyl alcohol derivative formation. Phytochemistry **66:** 2072–2091

Cresti M, Ciampolini DL, Mulcahy DL, Mulcahy GB (1985) Ultrastructure of *Nicotiana alata* pollen, its germination and early tube formation. Am J Bot **72:** 719–727

de Azevedo Souza C, Kim SS, Koch S, Kienow L, Schneider K, McKim SM, Haughn GW, Kombrink E, Douglas CJ (2009) A novel fatty acyl-CoA synthetase is required for pollen development and sporopollenin biosynthesis in *Arabidopsis*. Plant Cell **21:** 507–525

de Leeuw JW, Versteegh GJM, van Bergen PF (2006) Biomacromolecules of algae and plants and their fossil analogues. Plant Ecol **182:** 209–233

De Muyt A, Pereira L, Vezon D, Chelysheva L, Gendrot G, Chambon A, Lainé-Choinard S, Pelletier G, Mercier R, Nogué F, Grelon M (2009) A high throughput genetic screen identifies new early meiotic recombination functions in *Arabidopsis thaliana*. PLoS Genet **5:** e1000654

Dickinson HG, Sheldon JM (1986) The generation of patterning at the plasma membrane of the young microspore of *Lilium*. *In* S Blackmore, IK Ferguson, eds, Pollen and Spores: Form and Function, Vol 12. Academic Press, London, pp 1–17

Dieterle M, Zhou YC, Schäfer E, Funk M, Kretsch T (2001) EID1, an F-box protein involved in phytochrome A-specific light signaling. Genes Dev **15:** 939–944

Doan TTP, Carlsson AS, Hamberg M, Bülow L, Stymne S, Olsson P (2009) Functional expression of five Arabidopsis fatty acyl-CoA reductase genes in *Escherichia coli*. J Plant Physiol **166:** 787–796

Dobritsa AA, Lei Z, Nishikawa S, Urbanczyk-Wochniak E, Huhman DV, Preuss D, Sumner LW (2010) LAP5 and LAP6 encode anther-specific proteins with similarity to chalcone synthase essential for pollen exine development in Arabidopsis. Plant Physiol **153:** 937–955

Dobritsa AA, Nishikawa S, Preuss D, Urbanczyk-Wochniak E, Sumner LW, Hammond A, Carlson AL, Swanson RJ (2009a) LAP3, a novel plant protein required for pollen development, is essential for proper exine formation. Sex Plant Reprod **22:** 167–177

Dobritsa AA, Shrestha J, Morant M, Pinot F, Matsuno M, Swanson R, Møller BL, Preuss D (2009b) CYP704B1 is a long-chain fatty acid omega-hydroxylase essential for sporopollenin synthesis in pollen of Arabidopsis. Plant Physiol **151:** 574–589

Dong X, Hong Z, Sivaramakrishnan M, Mahfouz M, Verma DPS (2005) Callose synthase (CalS5) is required for exine formation during microgametogenesis and for pollen viability in Arabidopsis. Plant J **42:** 315–328

Douglas CJ (1996) Phenylpropanoid metabolism and lignin biosynthesis: from weeds to trees. Trends Plant Sci **1:** 171–178

Dover GA (1972) The organization and polarity of pollen mother cells of Triticum aestivum. J Cell Sci **11:** 699–711

Drakakaki G, Zabotina O, Delgado I, Robert S, Keegstra K, Raikhel N (2006) Arabidopsis reversibly glycosylated polypeptides 1 and 2 are essential for pollen development. Plant Physiol **142:** 1480–1492

Edlund AF, Swanson R, Preuss D (2004) Pollen and stigma structure and function: the role of diversity in pollination. Plant Cell (Suppl) **16:** S84–S97

Ehlting J, Büttner D, Wang Q, Douglas CJ, Somssich IE, Kombrink E (1999) Three 4-coumarate:coenzyme A ligases in Arabidopsis thaliana represent two evolutionarily divergent classes in angiosperms. Plant J **19:** 9–20

Faegri K, van der Pijl L (1979) The Principles of Pollination Ecology. Pergamon, Oxford

Fellenberg C, Böttcher C, Vogt T (2009) Phenylpropanoid polyamine conjugate biosynthesis in *Arabidopsis thaliana* flower buds. Phytochemistry **70:** 1392–1400

Fellenberg C, Milkowski C, Hause B, Lange PR, Böttcher C, Schmidt J, Vogt T (2008) Tapetum-specific location of a cation-dependent O-methyltransferase in *Arabidopsis thaliana*. Plant J **56:** 132–145

Fitzgerald MA, Knox RB (1995) Initiation of primexine in freeze-substituted microspores of *Brassica campestris*. Sex Plant Reprod **8:** 99–104

Forsbach A, Schubert D, Lechtenberg B, Gils M, Schmidt R (2003) A comprehensive characterization of single-copy T-DNA insertions in the *Arabidopsis thaliana* genome. Plant Mol Biol **52:** 161–176

Furness CA (2007) Why does some pollen lack apertures? A review of inaperturate pollen in eudicots. Bot J Linn Soc **155:** 29–48

Furness CA, Rudall PJ (2004) Pollen aperture evolution: a crucial factor for eudicot success? Trends Plant Sci **9:** 154–158

Grienenberger E, Besseau S, Geoffroy P, Debayle D, Heintz D, Lapierre C, Pollet B, Heitz T, Legrand M (2009) A BAHD acyltransferase is expressed in the tapetum of Arabidopsis anthers and is involved in the synthesis of hydroxycinnamoyl spermidines. Plant J **58:** 246–259

Grienenberger E, Kim SS, Lallemand B, Geoffroy P, Heintz D, Souza CdeA, Heitz T, Douglas CJ, Legrand M (2010) Analysis of TETRAKETIDE α-PYRONE REDUCTASE function in *Arabidopsis thaliana* reveals a previously unknown, but conserved, biochemical pathway in sporopollenin monomer biosynthesis. Plant Cell **22:** 4067–4083

Guan YF, Huang XY, Zhu J, Gao JF, Zhang HX, Yang ZN (2008) *RUPTURED POLLEN GRAIN1*, a member of the MtN3/saliva gene family, is crucial for exine pattern formation and cell integrity of microspores in Arabidopsis. Plant Physiol **147:** 852–863

Gubatz S, Herminghaus S, Meurer B, Strack D, Wiermann R (1986) The location of hydroxycinnamic acid amides in the exine of *Corylus* pollen. Pollen Spores **28:** 347–354

Guilford WJ, Schneider DM, Labovitz J, Opella SJ (1988) High resolution solid state C NMR spectroscopy of sporopollenins from different plant taxa. Plant Physiol **86:** 134–136

Häcker G (2000) The morphology of apoptosis. Cell Tissue Res **301:** 5–17

Hahlbrock K, Scheel D (1989) Physiology and molecular biology of phenylpropanoid metabolism. Annu Rev Plant Physiol Plant Mol Biol **40:** 347–369

Hellens RP, Edwards EA, Leyland NR, Bean S, Mullineaux PM (2000) pGreen: a versatile and flexible binary Ti vector for *Agrobacterium*-mediated plant transformation. Plant Mol Biol **42:** 819–832

Heslop-Harrison J (1963) An ultrastructural study of pollen wall ontogeny in *Silene pendula*. Grana Palynol **4:** 1–24

Heslop-Harrison J (1968a) Pollen wall development: the succession of events in the growth of intricately patterned pollen walls is described and discussed. Science **161:** 230–237

Heslop-Harrison J (1968b) Wall development within the microspore tetrad of *Lilium longiflorum*. Can J Bot **46:** 1185–1192

Heslop-Harrison J (1971) Wall pattern formation in angiosperm microsporogenesis. Symp Soc Exp Biol **25:** 277–300

Heslop-Harrison J (1979a) An interpretation of the hydrodynamics of pollen. Am J Bot **66:** 737–743

Heslop-Harrison J (1979b) Aspects of the structure, cytochemistry and germination of the pollen of rye. Ann Bot (Lond) **44:** 1–47

Heslop-Harrison J, Heslop-Harrison Y (1985) Germination of stress-tolerant *Eucalyptus* pollen. J Cell Sci **73:** 135–157

Heslop-Harrison Y, Heslop-Harrison J (1992) Germination of monocolpate angiosperm pollen evolution of the actin cytoskeleton and wall during hydration activation and tube emergence. Ann Bot (Lond) **69:** 385–394

Hird DL, Worrall D, Hodge R, Smartt S, Paul W, Scott R (1993) The anther-specific protein encoded by the *Brassica napus* and *Arabidopsis thaliana A6* gene displays similarity to beta-1,3-glucanases. Plant J **4:** 1023–1033

Hulskamp M, Parekh NS, Grini P, Schneitz K, Zimmermann I, Lolle SJ, Pruitt RE (1997) The *STUD* gene is required for male-specific cytokinesis after telophase II of meiosis in *Arabidopsis thaliana.* Dev Biol **187:** 114–124

Ito T, Shinozaki K (2002) The *MALE STERILITY1* gene of Arabidopsis, encoding a nuclear protein with a PHD-finger motif, is expressed in tapetal cells and is required for pollen maturation. Plant Cell Physiol **43:** 1285–1292

Katifori E, Alben S, Cerda E, Nelson DR, Dumais J (2010) Foldable structures and the natural design of pollen grains. Proc Natl Acad Sci USA **107:** 7635–7639

Kawakita M, Ishida N, Miura N, Sun-Wada G-H, Yoshioka S (1998) Nucleotide sugar transporters: elucidation of their molecular identity and its implication for future studies. J Biochem **123:** 777–785

Kim SS, Grienenberger E, Lallemand B, Colpitts CC, Kim SY, Souza CdeA, Geoffroy P, Heintz D, Krahn D, Kaiser M, et al (2010) LAP6/POLYKETIDE SYNTHASE A and LAP5/POLYKETIDE SYNTHASE B encode hydroxyalkyl α-pyrone synthases required for pollen development and sporopollenin biosynthesis in *Arabidopsis thaliana*. Plant Cell **22:** 4045–4066

Marrocco K, Zhou Y, Bury E, Dieterle M, Funk M, Genschik P, Krenz M, Stolpe T, Kretsch T (2006) Functional analysis of EID1, an F-box protein involved in phytochrome A-dependent light signal transduction. Plant J **45:** 423–438

Matsuno M, Compagnon V, Schoch GA, Schmitt M, Debayle D, Bassard JE, Pollet B, Hehn A, Heintz D, Ullmann P, et al (2009) Evolution of a novel phenolic pathway for pollen development. Science **325:** 1688–1692

McElver J, Tzafrir I, Aux G, Rogers R, Ashby C, Smith K, Thomas C, Schetter A, Zhou Q, Cushman MA, et al (2001) Insertional mutagenesis of genes required for seed development in *Arabidopsis thaliana*. Genetics **159:** 1751–1763

Meyers BC, Tej SS, Vu TH, Haudenschild CD, Agrawal V, Edberg SB, Ghazal H, Decola S (2004) The use of MPSS for whole-genome transcriptional analysis in Arabidopsis. Genome Res **14:** 1641–1653

Michelmore RW, Paran I, Kesseli RV (1991) Identification of markers linked to disease-resistance genes by bulked segregant analysis: a rapid method to detect markers in specific genomic regions by using segregating populations. Proc Natl Acad Sci USA **88:** 9828–9832

Mo Y, Nagel C, Taylor LP (1992) Biochemical complementation of chalcone synthase mutants defines a role for flavonols in functional pollen. Proc Natl Acad Sci USA **89:** 7213–7217

Morant M, Jørgensen K, Schaller H, Pinot F, Møller BL, Werck-Reichhart D, Bak S (2007) CYP703 is an ancient cytochrome P450 in land plants catalyzing in-chain hydroxylation of lauric acid to provide building blocks for sporopollenin synthesis in pollen. Plant Cell **19:** 1473–1487

Muller J (1979) Form and function in angiosperm pollen. Ann Miss Bot Gard **66:** 593–632

Napoli CA, Fahy D, Wang HY, Taylor LP (1999) *white anther*: a petunia mutant that abolishes pollen flavonol accumulation, induces male sterility, and is complemented by a chalcone synthase transgene. Plant Physiol **120:** 615–622

Nishikawa S, Zinkl GM, Swanson RJ, Maruyama D, Preuss D (2005) Callose (beta-1,3 glucan) is essential for Arabidopsis pollen wall patterning, but not tube growth. BMC Plant Biol **5:** 22

Owen HA, Makaroff CA (1995) Ultrastructure of microsporogenesis and microgametogenesis in *Arabidopsis thaliana* (L.) Heynh. ecotype Wassilewskija (Brassicaceae). Protoplasma **185:** 7–21

Paxson-Sowders DM, Dodrill CH, Owen HA, Makaroff CA (2001) DEX1, a novel plant protein, is required for exine pattern formation during pollen development in Arabidopsis. Plant Physiol **127:** 1739–1749

Paxson-Sowders DM, Owen HA, Makaroff CA (1997) A comparative ultrastructural analysis of exine pattern development in wild-type Arabidopsis and a mutant defective in pattern formation. Protoplasma **198:** 53–65

Perez-Munoz CA, Webster BD, Jernstedt JA (1995) Spatial congruence between exine pattern, microtubules and endomembranes in *Vigna* pollen. Sex Plant Reprod **8:** 147–151

Piffanelli P, Ross JHE, Murphy DJ (1998) Biogenesis and function of the lipidic structures of pollen grains. Sex Plant Reprod **11:** 65–80

Pollard M, Beisson F, Li Y, Ohlrogge JB (2008) Building lipid barriers: biosynthesis of cutin and suberin. Trends Plant Sci **13:** 236–246

Polowick PL, Sawhney VK (1995) Ultrastructure of the tapetal cell wall in the *stamenless-2* mutant of tomato (*Lycopersicon esculentum*): correlation between structure and male-sterility. Protoplasma **189:** 249–255

Quilichini TD, Friedmann MC, Samuels AL, Douglas CJ (2010) ATP-binding cassette transporter G26 is required for male fertility and pollen exine formation in Arabidopsis. Plant Physiol **154:** 678–690

Rhee SY, Osborne E, Poindexter PD, Somerville CR (2003) Microspore separation in the *quartet 3* mutants of Arabidopsis is impaired by a defect in a developmentally regulated polygalacturonase required for pollen mother cell wall degradation. Plant Physiol **133:** 1170–1180

Rollins RC, Banerjee UC (1979) Pollens of the Cruciferae. Bussey Institution, Harvard University, Cambridge, MA

Roshchina VV (2003) Autofluorescence of plant secreting cells as a biosensor and bioindicator reaction. J Fluoresc **13:** 403–420

Rowley JR, Dahl AO (1977) Pollen development in *Artemisia vulgaris* with special reference to glycocalix material. Pollen Spores **19:** 169–284

Rozema J, Broekman RA, Blokker P, Meijkamp BB, de Bakker N, van de Staaij J, van Beem A, Ariese F, Kars SM (2001) UV-B absorbance and UV-B absorbing compounds (para-coumaric acid) in pollen and sporopollenin: the perspective to track historic UV-B levels. J Photochem Photobiol B **62:** 108–117

Sanders PM, Bui AQ, Weterings K, McIntire KN, Hsu Y-C, Lee PY, Truong MT, Beals TP, Goldberg RB (1999) Anther developmental defects in *Arabidopsis thaliana* male-sterile mutants. Sex Plant Reprod **11:** 297–322

Schulze Osthoff K, Wiermann R (1987) Phenols as integrated compounds of sporopollenin from *Pinus* pollen. J Plant Physiol **131:** 5–15

Scott RJ (1994) Pollen exine: the sporopollenin enigma and the physics of pattern. *In* RJ Scott, AD Stead, eds, Molecular and Cellular Aspects of Plant Reproduction. University Press, Cambridge, UK, pp 49–81

Scott RJ, Spielman M, Dickinson HG (2004) Stamen structure and function. Plant Cell (Suppl) **16:** S46–S60

Sessions A, Burke E, Presting G, Aux G, McElver J, Patton D, Dietrich B, Ho P, Bacwaden J, Ko C, et al (2002) A high-throughput *Arabidopsis* reverse genetics system. Plant Cell **14:** 2985–2994

Sheldon JM, Dickinson HG (1983) Determination of patterning in the pollen wall of *Lilium henryi*. J Cell Sci **63:** 191–208

Sheldon JM, Dickinson HG (1986) Pollen wall formation in *Lilium*: the effect of chaotropic agents, and the organisation of the micro-tubular cytoskeleton during pattern development. Planta **168:** 11–23

Spielman M, Preuss D, Li FL, Browne WE, Scott RJ, Dickinson HG (1997) *TETRASPORE* is required for male meiotic cytokinesis in *Arabidopsis thaliana*. Development **124:** 2645–2657

Suzuki T, Masaoka K, Nishi M, Nakamura K, Ishiguro S (2008) Identification of *kaonashi* mutants showing abnormal pollen exine structure in *Arabidopsis thaliana*. Plant Cell Physiol **49:** 1465–1477

Takahashi M (1995) 3-Dimensional aspects of exine initiation and development in *Lilium longiflorum* (Liliaceae). Am J Bot **82:** 847–854

Takahashi M, Skvarla JJ (1991) Exine pattern formation by plasma membrane in *Bougainvillea spectabilis* Willd. (Nyctaginaceae). Am J Bot **78:** 1063–1069

Takeda S, Tadele Z, Hofmann I, Probst AV, Angelis KJ, Kaya H, Araki T, Mengiste T, Mittelsten Scheid O, Shibahara K, et al (2004) *BRU1*, a novel link between responses to DNA damage and epigenetic gene silencing in Arabidopsis. Genes Dev **18:** 782–793

Tang LK, Chu H, Yip WK, Yeung EC, Lo C (2009) An anther-specific dihydroflavonol 4-reductase-like gene (*DRL1*) is essential for male fertility in Arabidopsis. New Phytol **181:** 576–587

van der Veen JH, Wirtz P (1968) EMS-induced genic male sterility in *Arabidopsis thaliana*: a model selection experiment. Euphytica **17:** 371–377

Vizcay-Barrena G, Wilson ZA (2006) Altered tapetal PCD and pollen wall development in the Arabidopsis *ms1* mutant. J Exp Bot **57:** 2709–2717

von Besser K, Frank AC, Johnson MA, Preuss D (2006) Arabidopsis *HAP2* (*GCS1*) is a sperm-specific gene required for pollen tube guidance and fertilization. Development **133:** 4761–4769

Wehling K, Niester C, Boon JJ, Willemse MTM, Wiermann R (1989) p-Coumaric acid: a monomer in the sporopollenin skeleton. Planta **179:** 376–380

Wiermann R, Ahlers F, Schmitz-Thom I (2001) Sporopollenin. *In* A Stenbüchel, M Hofrichter, eds, Biopolymers, Vol 1. Wiley-VCH Verlag, Weinheim, Germany, pp 209–227

Wilson ZA, Morroll SM, Dawson J, Swarup R, Tighe PJ (2001) The Arabidopsis *MALE STERILITY1* (*MS1*) gene is a transcriptional regula-

tor of male gametogenesis, with homology to the PHD-finger family of transcription factors. Plant J **28:** 27–39

Wodehouse RP (1935) Pollen Grains: Their Structure, Identification and Significance in Science and Medicine. McGraw-Hill, New York

Worrall D, Hird DL, Hodge R, Paul W, Draper J, Scott R (1992) Premature dissolution of the microsporocyte callose wall causes male sterility in transgenic tobacco. Plant Cell **4:** 759–771

Wu A-M, Hörnblad E, Voxeur A, Gerber L, Rihouey C, Lerouge P, Marchant A (2010) Analysis of the Arabidopsis *IRX9/IRX9-L* and *IRX14/IRX14-L* pairs of glycosyltransferase genes reveals critical contributions to biosynthesis of the hemicellulose glucuronoxylan. Plant Physiol **153:** 542–554

Yang X, Makaroff CA, Ma H (2003) The *Arabidopsis MALE MEIOCYTE DEATH1* gene encodes a PHD-finger protein that is required for male meiosis. Plant Cell **15:** 1281–1295

Zimmermann P, Hirsch-Hoffmann M, Hennig L, Gruissem W (2004) GENEVESTIGATOR: Arabidopsis microarray database and analysis toolbox. Plant Physiol **136:** 2621–2632

Zinkl GM, Preuss D (2000) Dissecting Arabidopsis pollen-stigma interaction reveals novel mechanisms that confer mating specificity. Ann Bot (Lond) **85:** 15–21

Zinkl GM, Zwiebel BI, Grier DG, Preuss D (1999) Pollen-stigma adhesion in Arabidopsis: a species-specific interaction mediated by lipophilic molecules in the pollen exine. Development **126:** 5431–5440